

Research Article

Nucleation Capacity and Presence of Centrioles Define a Distinct Category of Centrosome Abnormalities that Induces Multipolar Mitoses in Cancer Cells

Michael J. Difilippantonio,^{1*} B. Michael Ghadimi,¹ Tamara Howard,² Jordi Camps,¹ Quang Tri Nguyen,¹ Douglas K. Ferris,³ Dan L. Sackett,⁴ and Thomas Ried¹

¹Genetics Branch, Center for Cancer Research, NCI/NIH, Bethesda, Maryland

²Department of Cell Biology and Physiology, University of New Mexico - Health Sciences Center, Albuquerque, New Mexico

³SAIC, Basic Research Laboratory, FCRDC, NCI/NIH, Bethesda, Maryland

⁴Laboratory of Integrative and Medical Biophysics, Program in Physical Biology NICHD/NIH, Bethesda, Maryland

Analysis of centrosome number and structure has become one means of assessing the potential for aberrant chromosome segregation and aneuploidy in tumor cells. Centrosome amplification directly causes multipolar catastrophic mitoses in mouse embryonic fibroblasts (MEFs) deficient for the tumor suppressor genes *Brcal* or *Trp53*. We observed supernumerary centrosomes in cell lines established from aneuploid, but not from diploid, colorectal carcinomas; however, multipolar mitoses were never observed. This discrepancy prompted us to thoroughly characterize the centrosome abnormalities in these and other cancer cell lines with respect to both structure and function. The most striking result was that supernumerary centrosomes in aneuploid colorectal cancer cell lines were unable to nucleate microtubules, despite the presence of γ -tubulin, pericentrin, PLK1, and AURKA. Analysis by scanning electron microscopy revealed that these supernumerary structures are devoid of centrioles, a result significantly different from observations in aneuploid pancreatic cancer cell lines and in *Trp53* or *Brcal* deficient MEFs. Thus, multipolar mitoses are dependent upon the ability of extra γ -tubulin containing structures to nucleate microtubules, and this correlated with the presence of centrioles. The assessment of centrosome function with respect to chromosome segregation must therefore take into consideration

the presence of centrioles and the capacity to nucleate microtubules. The patterns and mechanisms of chromosomal aberrations in hematologic malignancies and solid tumors are fundamentally different. The former is characterized by specific chromosome translocations, whose consequence is the activation of oncogenes. Most carcinomas, however, reveal variations in the nuclear DNA content. The observed genomic imbalances and gross variations in chromosome number can result from unequal chromosome segregation during mitotic cell division. It is therefore fundamental to elucidate mechanisms involved in distribution of the genome to daughter cells. Prior to cell division, the centrosome organizes microtubules and the mitotic spindle. Deciphering the consequences of alterations in centrosome number, structure, and function is an important step towards understanding how a diploid genome is maintained. Although extra centrosomes have now been observed in carcinomas and were correlated with aneuploidy, a careful functional investigation of these structures and their role in generating chromosome imbalances may lead to the identification of distinct mechanistic pathways of genomic instability. Understanding these pathways will also be important in determining whether they are potential molecular targets of therapeutic intervention. Environ. Mol. Mutagen. 50:672–696, 2009. © 2009 Wiley-Liss, Inc.

Key words: centrosome; aneuploidy; chromosome instability; gene expression

Grant sponsor: This work was supported in part by the Intramural Research Program of the NIH, National Cancer Institute, Center for Cancer Research and by the Intramural Research Program of the Eunice Kennedy Shriver National Institute of Child Health and Human Development, NIH.

*Correspondence to: Michael J. Difilippantonio, 50 South Drive, Rm 1408, Bethesda, MD 20892, USA. E-mail: difilipm@mail.nih.gov

Received 28 May 2009; Provisionally accepted 12 August 2009; and in final form 13 August 2009

DOI 10.1002/em.20532

Published online 20 September 2009 in Wiley InterScience (www.interscience.wiley.com).

INTRODUCTION

Over a century ago, Theodor Boveri coined the term centrosome to describe the subcellular structures originally observed by Van Beneden in 1876. He postulated that due to their role in cell division, deviation in number from the two centrosomes normally present in each cell could have dire consequences with respect to the partitioning of chromosomes into the daughter cells. Subsequent chromosome missegregation could result in the loss of tumor inhibiting, and the gain of tumor promoting, chromosomes and that this served as the genetic basis of malignant transformation [Boveri, 1929]. The development of molecular cytogenetic techniques [Kallioniemi et al., 1992; Schröck et al., 1996], and their recent adaptation to higher resolution platforms including whole genome sequencing [Dufva, 2009; Pettersson et al., 2009], has enabled the comprehensive characterization of chromosomal aberrations in cancer genomes. It has become clear through the use of these techniques that solid tumors originating in epithelial cells of different organs are characterized by a distribution of specific and distinct genomic imbalances, that whole chromosome gains and losses are early events in tumorigenesis [Ried et al., 1999] and that strong selection for these events may have a causative role in tumorigenesis. Accordingly, Boveri's hypothesis with respect to chromosome segregation errors and the role of centrosomes in this process has been revisited [Brinkley and Goepfert, 1998; Pihan et al., 1998; Pihan and Doxsey, 1999; Ried, this issue].

The centrosome is positioned in the cytoplasm adjacent to the nucleus and its duplication is concurrent with replication of the genome during S phase. At the beginning of M phase, the two centrosomes separate to opposite poles of the nucleus where they nucleate the formation of mitotic spindles containing α - and β -tubulin, many of which eventually connect to kinetochore proteins associated with the centromere of each chromosome. A dynamic interplay between the microtubules, mitotic kinesins, and cytokinesins is necessary for the coordinated separation of sister chromatids, their migration to opposite poles and generation of the cleavage furrow at the end of mitosis [Brinkley, 2001; Stearns, 2001; Bowerman, 2004; Rogers et al., 2004; Neef et al., 2006; Petronczki et al., 2007].

Centrosomes consist of centrioles and the pericentriolar matrix (PCM). The centrioles contain a protein known as centrin, while the PCM contains γ -tubulin, pericentrin (PCNT), hGCP2, GCP3/HsSpc98, and AKAP450 among other proteins too numerous to list [Brinkley, 2001; Stearns, 2001; Alieva and Uzbekov, 2008]. Two protein families shown to regulate centrosome duplication and/or separation are the polo-like kinases (e.g., PLK1) and aurora family kinases (e.g., AURKA) [Glover et al., 1995; Lane and Nigg, 1996]. Overexpression of these proteins

results in supernumerary centrosomes, while abrogating expression causes a failure of centrosome migration [Lane and Nigg, 1996; Zhou et al., 1998]. The Cdk2-cyclin E (Cdk2-E) complex has been shown to regulate centrosome duplication in *Xenopus* cell extracts [Hinchcliffe et al., 1999]. A positive feedback loop between the *Xenopus* Plk1 protein (Plx1) and a downstream protein kinase target xPlkk1 has also been demonstrated [Qian et al., 1998a,b; Erikson et al., 2004], implicating yet another phosphorylation pathway regulating the centrosome cycle.

We and others have previously demonstrated the presence of supernumerary centrosomes in primary tumors and tumor cell lines of different origins [Lingle et al., 1998; Pihan et al., 1998; Ghadimi et al., 2000]. These findings have been touted as proof that extra centrosomes can cause aneuploidy through their direct role in missegregation of chromosomes during mitosis. In only a very few instances, however, has this mechanism been proven by direct visualization of aberrant mitotic figures [Fukasawa et al., 1996; Xu et al., 1999]. In this study, we have identified differences with respect to the type of centrosome aberrations occurring in tumorigenesis. Our results suggest that the failure of certain centrosomes to nucleate microtubules and organize the mitotic spindle could be due to the absence of centrioles. This is the first report to our knowledge of γ -tubulin structures lacking nucleation capacity in mammalian cells.

EXPERIMENTAL PROCEDURES

Cell Lines and RNA Isolation

The following colorectal cancer cell lines were used in this study: DLD-1, HCT116, p53HCT116, SW48, and LoVo (near-diploid); SW480, SW837, HT-29, T84, Colo 201 for immunocytochemistry and nucleation assays. For gene expression analysis Colo 320DM, LS411N, SK-CO-1, NCI-H508, and NCI-H716 (aneuploid) were also used. The pancreatic tumor cell lines included AsPC-1, BxPC-3, Capan-1, Capan-2, CFPac-1, Hs766T, Mia PaCa-2, Panc-1, SU 86.86. All of the aforementioned cell lines were obtained from the ATCC (American Type Culture Collection) and cultured following their recommendations, except p53HCT116, a derivative of HCT116 with a homozygous disruption of *TP53* [Bunz et al., 1998], which was kindly provided by Dr. Curtis C. Harris of the National Cancer Institute, NIH. Control fibroblasts were cultured from human foreskin. p53 $^{-/-}$ mouse embryonic fibroblasts (MEFs) were obtained from Andre Nussenzweig of the National Cancer Institute, NIH.

RNA was extracted from the cell lines and primary tumors [Camps et al., 2009] following standard procedures (<http://www.riedlab.nci.nih.gov/protocols.asp>). Nucleic acid quantification was determined using the Nanodrop ND-1000 UV-VIS spectrophotometer (Nano-

drop, Rockland, DE), and RNA quality was assessed using the Bioanalyzer 2100 (Agilent Technologies, Santa Clara, CA). Normal colon RNA isolated postmortem from five different donors without a history of colorectal cancer was purchased from Ambion (Applied Biosystems, Foster City, CA).

Antibodies

Mouse monoclonal antibodies were used to detect γ -tubulin (Sigma-Aldrich, St Louis, MO, T6557; diluted 1:2,000) and α -tubulin (Sigma-Aldrich, T9026; diluted 1:1,000). Anti-PCNT rabbit polyclonal antibodies were obtained from Berkley Ab Company, Berkley, CA (PRB-432C; diluted 1:100). Anti-PLK1 and anti-AURKA rabbit polyclonal antibodies were produced by injection of peptide [Hamanaka et al., 1995]. Secondary antibodies used for immunocytochemistry were purchased from Vector Laboratories, Burlingame, CA (Goat anti-rabbit-TR, TI-1000, diluted 1:1,000) and Boehringer Mannheim, Indianapolis, IN (Goat anti-mouse-FITC, diluted 1:200).

Immunocytochemistry

Cells were grown on Falcon chamber slides (Becton & Dickinson, Bedford, MA), rinsed once each in PBS and PHEM buffer [PIPES (60 mM), HEPES (25 mM), EGTA (10 mM), MgCl₂ (2 mM), pH 6.9], fixed in ice cold methanol for 10 min and washed 4 \times with PBS. Slides were blocked with 5% normal goat serum (NGS), 1% BSA in PBS for 30 min at 37°C. Primary antibodies were diluted (as indicated above) in 1% NGS, 1% BSA in PBS and incubated for 45 min at 37°C followed by three washes in PBS. The primary antibodies were detected with goat anti-rabbit-TR and goat anti-mouse-FITC followed by three washes in PBS. Cells were counterstained with DAPI and mounted with antifade [*p*-phenylene-diamine (5.52 mM), 77% glycerol, 0.1 \times PBS, at pH 8.0 with carbonate/bicarbonate buffer (pH 9.0)]. Images were acquired using Leica Q-FISH software (Leica Imaging Systems, Cambridge, UK). A minimum of 50 mitotic figures and 300 interphase nuclei were evaluated for centrosome number and organization.

Nucleation Assays

Cell lines were grown on Falcon culture slides (Becton & Dickinson). Cells were then incubated with the microtubule destabilizing drug nocodazole (10 μ g/ml) for 1.5 hr at 37°C, and washed two times with PBS at room temperature and allowed to recover by incubation in media for 5–10 min. Slides were then rinsed once in PBS, once with PHEM buffer and then fixed in –20°C methanol. Tubulin structures were detected by incubating cells with a monoclonal α -tubulin (Sigma-Aldrich, 1:1,000) and rabbit polyclonal γ -tubulin (Sigma-Aldrich, 1:2,000) antibodies for 45 min. Following three PBS washes, the primary antibodies were detected with a FITC labeled goat anti-mouse and a TRITC labeled

goat anti-rabbit antibody (Sigma-Aldrich, 1:200 each) for 45 min, and cells were counterstained with DAPI.

Standard Transmission Electron Microscopy and Immunoelectron Microscopy

Cultured cells were processed *in situ* and embedded for electron microscopy as described [Gonda et al., 1976]. Briefly, cells were cultured in a T-75 flask, rinsed once with PBS and fixed with sodium cacodylate buffer (0.1 M, pH 7.2) (Electron Microscope Sciences, Fort Washington, PA) containing 2% glutaraldehyde (Tousimis, Rockville, MD) for 1 hr at room temperature. The fixed cells were then rinsed with cacodylate buffer followed by post-fixation in cacodylate buffer + 1% osmium tetroxide (Electron Microscope Sciences, Fort Washington, PA) for 1 hr. The cells were dehydrated in an ethanol series (35, 50, 70, 95, and 100%) with three changes of absolute ethanol, embedded in pure Embed-812 epoxy resin (Electron Microscope Sciences, Fort Washington, PA) overnight and allowed to cure for 48 hr at 55°C. Ultra-thin sections were cut and mounted on copper grids and stained with uranyl acetate followed by lead citrate. The sections were observed and photographed using a Hitachi H-7000 transmission electron microscope (Nissei Sanyo America, Pleasanton, CA) operated at 75 kV.

For ICC/EM, cells were cultured on gridded glass coverslips (22 \times 22 mm²) (Bellco Biotechnology, Vineland, NJ) and washed in PBS. The cells were fixed in cytoskeletal buffer (CSK) [PIPES (910 mM), NaCl (100 mM), sucrose (300 mM), EGTA (1 mM), MgCl₂ (3 mM)] + 0.1% Triton X-100 for 30 min, CSK + 0.1% Triton X-100 + 1% glutaraldehyde for 2 min and CSK + 0.1% glutaraldehyde for 10 min. This was followed by two 15 min treatments with 0.1% NaBH₄ in PBS. The coverslips were then processed for immunofluorescence as stated above using mouse mAb against γ -tubulin detected with goat anti-mouse-FITC and counterstained with DAPI. Images were acquired of cells with aberrant numbers of γ -tubulin staining bodies using a Nikon FXA fluorescence microscope and their coordinates recorded. The coverslips were floated off the slides and washed several times in PBS and then immersed in PBS overnight at 4°C. The cells were then washed 2 \times 5 min in PBS and followed by 3 \times 5 min washes in 0.1 M sodium cacodylate buffer (pH 7.0). Cells were postfixed in 1% osmium potassium ferrocyanide for 1 hr at room temperature, washed 2 \times 5 min in 0.1 M sodium cacodylate and then 2 \times 5 min in dH₂O. Samples were stained with 2% aqueous uranyl acetate for 30 min at room temp, washed 3 \times 5 min in dH₂O, dehydrated in ethanol, and infiltrated and embedded in Epon/Araldite. Thin sections were cut, and the cells were relocated by their coordinates and examined using a Hitachi H-7000 transmission electron microscope [Nissei Sanyo America, Pleasanton, CA] operated at 75 kV.

Gene Expression Microarrays and Data Analysis

The procedure followed for the hybridization and analysis of the gene expression arrays can be found elsewhere for the primary tumors [Camps et al., 2008] and the CRC cell lines [Camps et al., 2009]. Briefly, 1 µg each of cell line or normal human colon RNA (Ambion, Austin, TX) and Universal Human Reference RNA (Stratagene, Cedar Creek, TX) were amplified and labeled with Cy3 and Cy5, respectively, using a T7 RNA Polymerase (Low RNA Input Fluorescent Linear Amplification Kit, Agilent) according to the manufacturer's protocols, and hybridized to the 44K oligonucleotide-based Whole Human Genome Microarray (Agilent). Similarly, RNA from primary tumors and normal human colon were labeled with Cy3 and subjected to mono-channel hybridization onto 4x44K Whole Human Genome Microarray (Agilent).

Microarrays were washed and processed using an Agilent G2565BA laser scanner. Data were quality controlled and extracted using Agilent Technologies' Feature Extraction (version 9.1).

The analyses of the microarray experiments were performed with in-house developed software based on R version 2.6.2 (<http://www.R-project.org>). Gene expression data was obtained from 44K or 4x44K Agilent dual-channel arrays. Median per feature was used to summarize data when two or three technical replicates were available. The data were normalized using Linear and Lowess procedure in Agilent's Feature Extraction software. Features for which signals were below background (as assessed by "gSurrogatedUsed" or "rSurrogatedUsed") were forced to NA (not a number). The median measurement was used when more than 1 measurement was available per feature (i.e., median-summarization by array using "ProbeName"). The final CRC cell line dataset contained 20 samples (15 cell lines, and five normal colon samples), and 40,380 features.

RESULTS

Numerical Aberrations

Diploid and aneuploid colorectal tumor cell lines show striking differences with respect to both centrosome number and structure [Ghadimi et al., 2000]. Despite the presence of supernumerary centrosomes in the aneuploid tumors, we fail to observe a potential consequence of centrosome amplification, i.e., multipolar mitoses. We therefore began a thorough functional and structural analysis of centrosomes in normal cultured foreskin fibroblast cells, diploid tumors, and aneuploid tumors with and without multipolar mitoses. On the basis of these analyses, we identified distinct differences in the number, size, and localization of the centrosomes in these cell types.

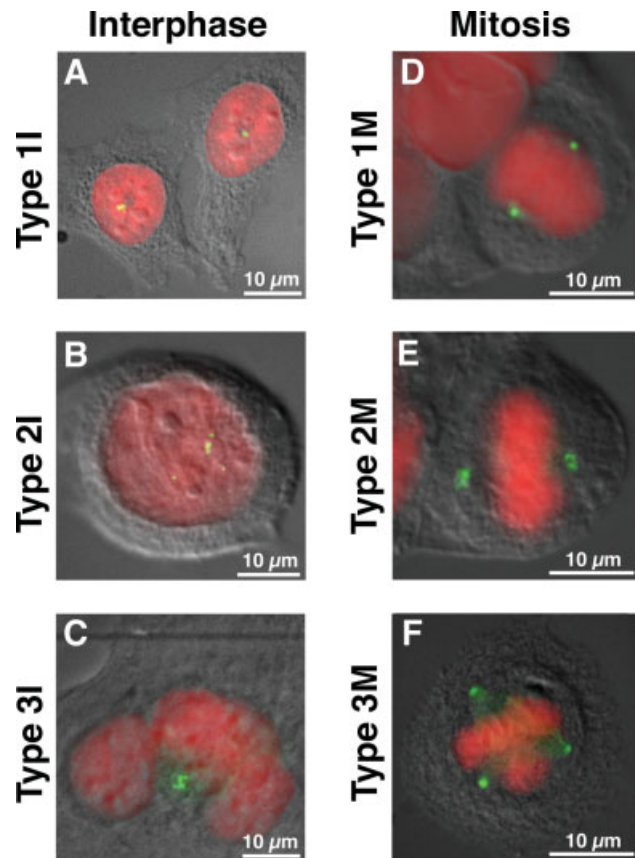


Fig. 1. Interphase cells (I) were categorized based on the number of their centrosomes (green) as detected with an anti- γ -tubulin antibody. DNA was counterstained with DAPI (red) and the cells visualized by differential interference contrast (DIC) microscopy. Type 1I (A) have one to two centrosomes. Type 2I (B) are mononucleated cells with multiple centrosomes while Type 3I (C) contain multiple centrosomes in a multinucleated cell. Mitotic cells (M) were categorized in a similar manner based on the number and orientation of their centrosomes with respect to the mitotic plate. Type 1M (D) have a bipolar spindle with one centrosome on either side of the mitotic plate. Type 2M (E) mitoses are bipolar but demonstrate coalescence of multiple centrosomes at either pole. Type 3M (F) are multipolar mitoses in which the chromosomes are pulled in more than two directions.

Normal fibroblasts, as well as the diploid colorectal cell lines (HCT116, DLD1, SW48), contained 1-2 γ -tubulin positive staining bodies resulting in the formation of a normal bipolar mitosis (Figs. 1A and 1D). The aneuploid colorectal cell lines (HT29, SW837, SW480, Colo201, and T84) each had a subpopulation of cells containing ≥ 3 γ -tubulin positive bodies [Ghadimi et al., 2000], the size and morphology of which was variable (Fig. 1B: mono-nucleated or Fig. 1C: multinucleated cells). All of the observed mitoses were bipolar, however, with some exhibiting clusters of γ -tubulin at the poles (Fig. 1E). We therefore extended our analysis of centrosome defects to include aneuploid cancer cell lines of pancreatic origin.

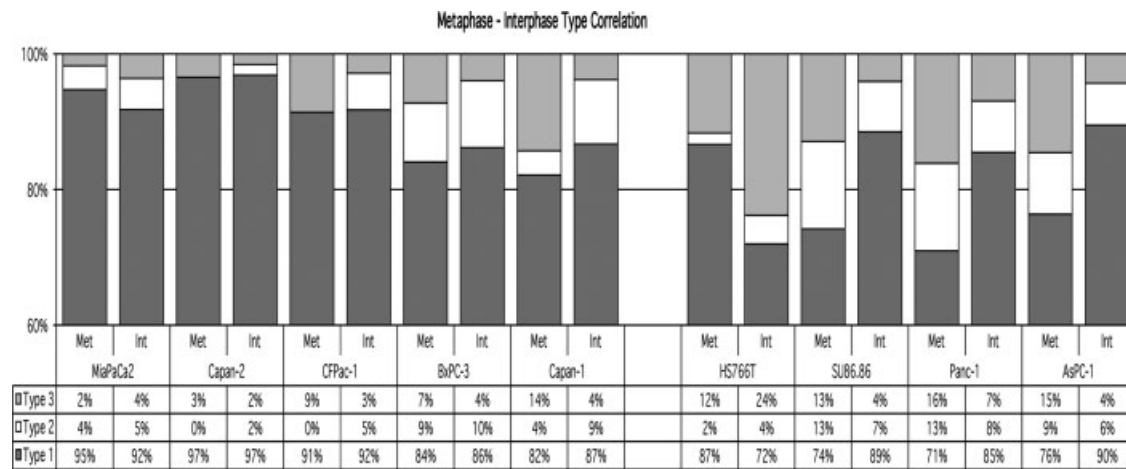


Fig. 2. Quantitation and comparison of interphase (Int) ($n \geq 300$) and metaphase (Met) ($n \geq 50$) pancreatic cancer cells based on the categories illustrated in Figure 1.

These lines also contained a percentage of cells with an abnormal number of γ -tubulin positive structures (Table I); however, all were of equal size and morphology, a phenotype distinct from the colorectal cancer cell lines. In addition, we frequently observed multipolar mitoses (Fig. 1F) (Fig. 2G).

Many of the aneuploid colorectal cancer cell lines contain inactivating *TP53* mutations. The pattern of interphase centrosome aberrations we observed was consistent with the centrosome amplification seen in *Trp53*–/– or *Brcal*–/– MEFs [Fukasawa et al., 1996; Xu et al., 1999]. This caused us to wonder whether *TP53* loss had a comparable consequence with respect to centrosome number in all cancer cell lines. To address this question, we took advantage of the diploid colorectal cancer cell line HCT116 made homozygously deficient for the *TP53* protein (p53HCT116) [Waldman et al., 1996]. Unlike the *TP53* wild-type parental cells, this cell line had centrosome amplification and multipolar mitoses akin to the *Trp53*–/– MEFs (see later).

Despite the absence of gross chromosome missegregation in the aneuploid colorectal cancer cell lines, we were interested in determining whether the interphase centrosome aberrations observed in the pancreatic cell lines could be directly correlated with events occurring during mitosis. A comparison of interphase and metaphase cell types in MiaPaCa2, Capan-2, CFPac-1, BxPC-3, and Capan-1 revealed that the percentage of interphase and metaphase cells with one to two centrosomes was similar (Fig. 2; Types 1I vs. 1M). Thus, the population of interphase cells with normal centrosome numbers correlated with the percentage of metaphase cells containing two centrosomes and normal bipolar mitotic spindles. This was not true, however, for HS766T, SU86.86, Panc-1, and AsPC-1 cells (Fig. 2).

TABLE I. Comparison of Centrosome Aberrations During Mitosis and Interphase in Pancreatic Cell Lines

Cell line	Interphase nuclei		Mitoses Observed multipolar ^b
	Observed abnormal ^a	Observed multipolar ^b	
AsPC-1	10%		15%
BxPC-3	14%		7%
Capan-1	13%		9%
Capan-2	3%		3%
CFPac-1	8%		9%
HS766T	28%		19%
Mia PaCa-2	8%		2%
Panc-1	15%		16%
SU86.86	11%		13%

^aType 2 and Type 3 interphase cells combined.

^bType 3 metaphase cells.

Functional Aberrations

α -tubulin staining of mitotic spindles in *Brcal*–/– and *Trp53*–/– MEFs and in p53HCT116 and pancreatic cancer cell lines (Table I; [Sato et al., 2001]), revealed multiple nucleating centrosomes and multipolar mitosis, structures associated with gross chromosomal missegregation. Aberrant mitoses, however, were not observed in the aneuploid colorectal cell lines, despite the presence of supernumerary γ -tubulin structures. This prompted us to assess whether all of the γ -tubulin structures in the aneuploid colorectal tumor cell lines were functionally capable of nucleating microtubules.

Nocodazole is a potent microtuble depolymerizing drug that causes cell cycle arrest at mitosis [Jordan et al., 1998]. The damage is reversible such that replacement with fresh medium allows repolymerization of the microtubules and the procession of mitosis. We therefore used nocodazole block and release to assess the ability of γ -tubulin structures to nucleate α -tubulin containing

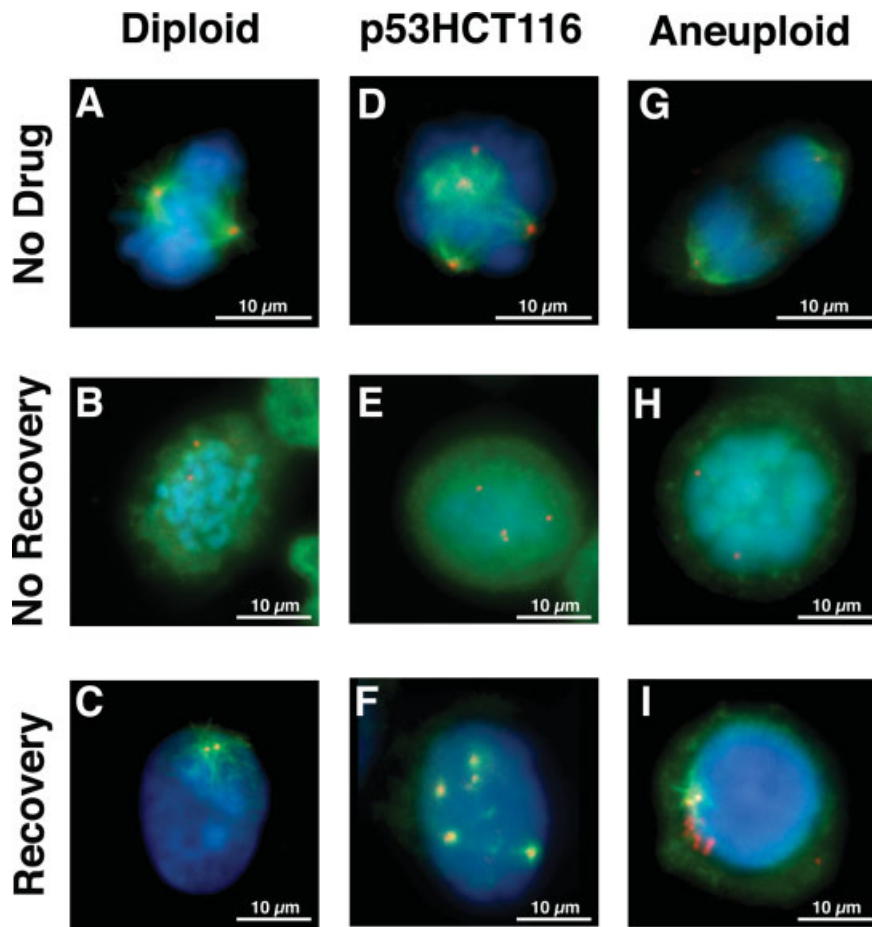


Fig. 3. Nucleation assay and subsequent detection of both α -tubulin spindles (green) and γ -tubulin (red) in diploid (A–C) and aneuploid (G–I) colorectal cancer cell lines as well as p53HCT116 (D–F), a diploid colorectal cell line made homozygous deficient for TP53. Untreated cells (A, D, G) in mitosis reveal mitotic spindles nucleating from the centrosomes. Nocodazole treated cells (B, E, H) in mitosis. The absence

of mitotic spindles demonstrates the microtubule depolymerizing activity of the drug. Cells allowed to briefly recover from nocodazole treatment (C, F, I) reveal nucleation of α -tubulin containing microtubules from all γ -tubulin structures in the diploid (C) and p53HCT116 (F) cells compared to only one to two γ -tubulin structures in the aneuploid colorectal cell lines (I).

microtubules. Efficient microtubule nucleation from centrosomes was most readily observed in mitotic cells in the absence of nocodazole (Figs. 3A, 3D, and 3G). The effectiveness of microtubule depolymerization by nocodazole can be seen in Figures 3B, 3E, and 3H. In the diploid colorectal cell lines and normal fibroblasts (Fig. 3C), p53HCT116 (Fig. 3F), pancreatic cancer cell lines and p53 $^{−/−}$ MEFs (data not shown), all γ -tubulin positive structures, regardless of their number, functioned as α -tubulin nucleating centers shortly after removal of nocodazole. This differed markedly from the aneuploid colorectal cancer cell lines in which, despite the presence of multiple γ -tubulin structures, only one to two centrosomes in each cell were observed to function as nucleating centers in the formation of normal mitotic spindles (Fig. 3I). Thus, the absence of multipolar mitoses in the aneuploid colorectal cancer cell lines correlated with the inability of

supernumerary centrosomes to serve as nucleation centers for α -tubulin containing mitotic spindles.

Structural Aberrations

In an effort to determine why these supernumerary structures were not capable of giving rise to multipolar mitosis, colocalization studies of γ -tubulin with other centrosome-associated proteins were performed. PLK1 is normally associated with centrosomes throughout the cell cycle, until anaphase when it relocates to the metaphase plate and is distributed as two rings at the midbody during cytokinesis [Lane and Nigg, 1996]. This pattern was recapitulated in both diploid (HCT116, p53HCT116, DLD1) and aneuploid (HT29, SW480, Colo201) CRC cell lines irrespective of the number of γ -tubulin positive structures. Representative images from different cell lines

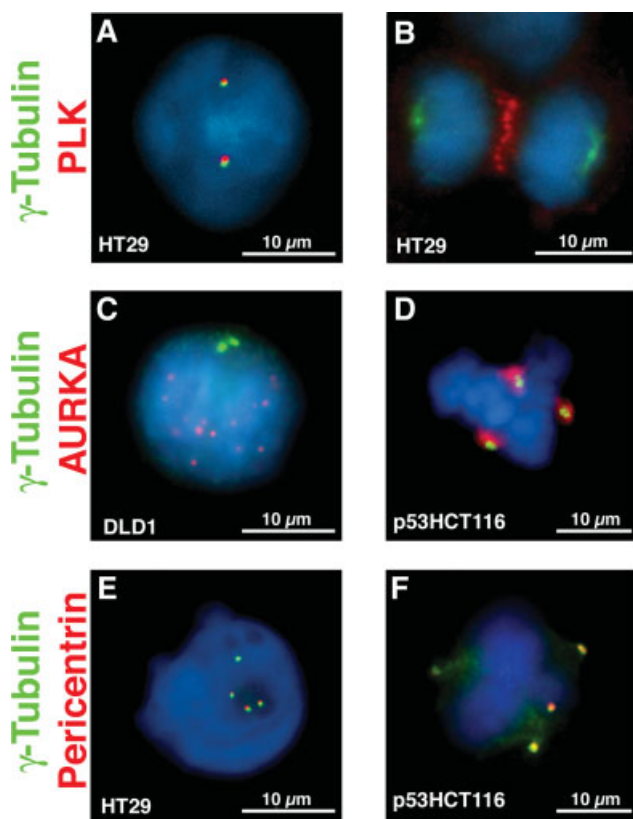


Fig. 4. Dual immunofluorescence for γ -tubulin and Polo-like kinase 1 (PLK1) (A, B), aurora-kinase A (AURKA) (C, D), and PCNT (E, F). Interphase cells reveal colocalization of γ -tubulin with PLK1 (A) and PCNT (E) but not with AURKA (C). In mitosis, however, all four protein colocalize (D, E), however PLK1 remains at the metaphase plate during anaphase (B) and is found as two rings at the midbody after cytokinesis.

are shown in Figures 4A and 4B. In interphase, AURKA is distributed in multiple, noncentrosomal nuclear foci. Its association with centrosomes only occurs during mitosis. This redistribution pattern was also recapitulated in all of the CRC cell lines analyzed (Figs. 4C and 4D), with AURKA localized to every γ -tubulin positive structure. PCNT, as part of the pericentriolar matrix (PCM), always colocalizes with γ -tubulin in centrosomes [Doxsey et al., 1994], as was the case in all of the analyzed cell lines (Figs. 4E and 4F). Thus, we found no difference in the centrosome-associated localization pattern of PLK1, AURKA, or PCNT proteins between diploid and aneuploid colorectal tumor cell lines. The presence of these centrosome-associated proteins was therefore insufficient to nucleate mitotic spindles and generate multipolar mitoses.

Each centrosome, as visualized by electron microscopy, consists of a pair of centrioles oriented at 90° relative to one another. Both fibroblasts and the diploid CRC cell line DLD1 contained one to two centrosomes, each with a

pair of appropriately oriented centrioles (Figs. 5A–5C). Many of the *Trp53*–/– MEFs and p53HCT116 cells contained multiple centriole pairs, often found in clusters (Figs. 5D–5F). This was not surprising given the normal association of PCNT, PLK1 and AURKA with all of the supernumerary γ -tubulin structures (Fig. 4) and the presence of multipolar mitoses in these cells (Figs. 3D and 4F). Examination of the aneuploid colorectal cancer cell lines revealed the presence of only one to two centriole pairs in greater than 95% of the cells (Figs. 5G–5I). In the remaining cells, clusters of centrioles were observed (Fig. 6L); however, the perpendicular orientation between pairs of centrioles was sometimes lost (data not shown).

This differed from our previous immunocytochemical observation that 30–40% of the SW837 cells contained multiple γ -tubulin structures. We therefore grew the cells on gridded coverslips, performed immunocytochemistry, identified those cells with multiple γ -tubulin structures and recorded their coordinates. The cells were then embedded for electron microscopy, serial sections cut and the cells relocated based on their coordinates. This afforded us the opportunity to directly correlate the presence of γ -tubulin and centrioles. As anticipated, all of the supernumerary centrosomes in the *Trp53*–/– MEFs contained a perpendicularly oriented pair of centrioles (Figs. 6A–6D). In the aneuploid SW837 cancer line, cells with multiple γ -tubulin structures were found to contain only one or two pairs of centrioles (Figs. 6E–6H), despite analysis of serial sections through the cells. Cells containing clusters of centrioles (Figs. 6I–6L) did not always aggregate all of their γ -tubulin in one location. Thus, we were greatly surprised to find that the supernumerary structures containing γ -tubulin, PCNT, and PLK in the aneuploid colorectal cancer cell lines were actually devoid of centrioles, thereby correlating the presence of centrioles with the nucleation capacity of γ -tubulin structures and the propensity for catastrophic multipolar mitoses.

Gene Expression Analysis

One approach to query the large number of genes currently known to be involved in centrosome regulation and function is global gene expression analysis. We expanded our set of CRC cell lines to include an additional five aneuploid CRC cell lines as well as five biopsies of normal colon epithelia. These results were also compared to a previous analysis consisting of 23 primary colon carcinomas [Camps et al., 2009]. Of the 121 genes spotted on the array that we queried based on their known or potential connection to the development of aneuploidy through an association with the centromere, centrosome, or spindles, 11 genes were significantly deregulated ($P < 0.0001$) in both the diploid and aneuploid cell lines relative to the mucosa, and of these seven were also of significance in primary colon tumors (Table II). Only *CSSP1*

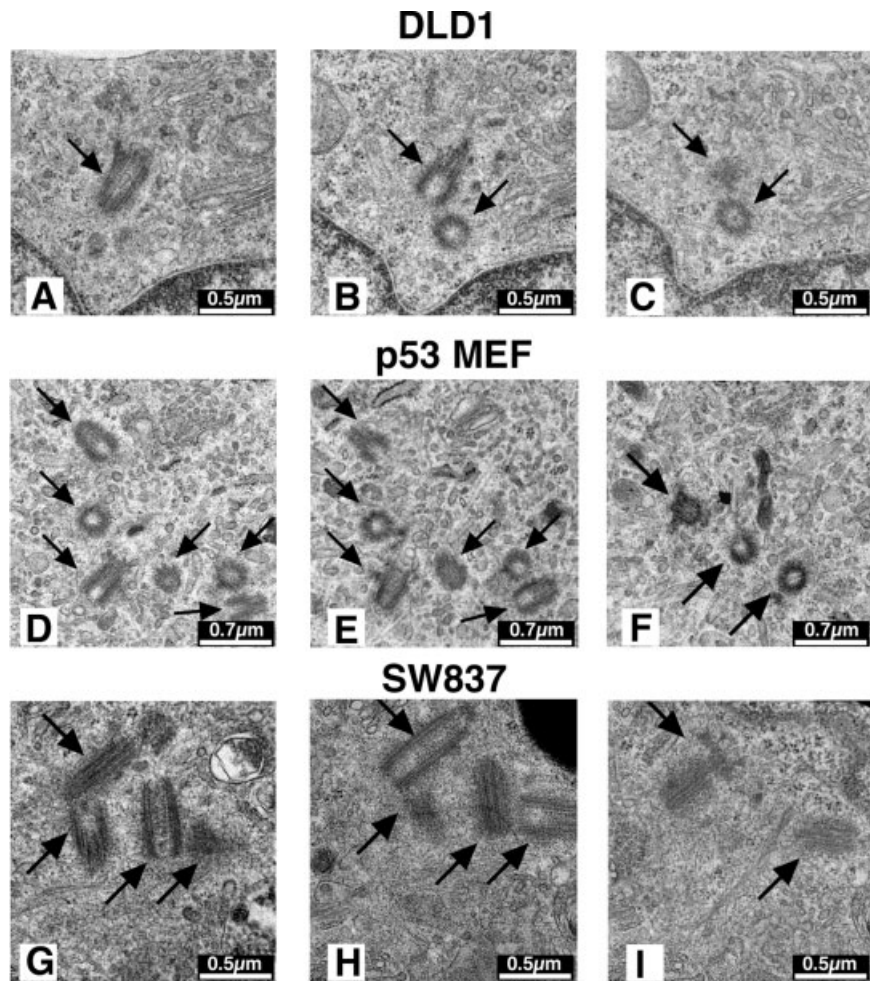


Fig. 5. Electron microscopic serial sections of centrioles. One centriole pair, in their normal perpendicular orientation, as illustrated in the diploid cell line DLD1 (A–C). In *Trp53*-deficient MEFs (D–F) and the *TP53*-deficient HCT116 cell line (data not shown), multiple pairs of cen-

trioles were observed, sometimes in clusters. Three pairs of centrosomes are depicted here. In the aneuploid colorectal cancer cell lines, such as shown for SW837 (G–I), two pairs of centrosomes were also observed, even in cells with multiple γ -tubulin foci.

(1.48- to 1.96-fold decrease, $P = 0.009$ – 0.0005), *CETN2* (2.23-fold increase, $P = 0.000104$), *TTL4* (1.4-fold increase, $P = 0.009$), and *TUBGCP6* (1.52-fold decrease, $P = 0.0039$) had an expression difference that reached any significance ($P < 0.01$) in the aneuploid relative to the diploid cell lines.

DISCUSSION

In an effort to understand the causal events leading to the development of aneuploidy in tumorigenesis, we have undertaken a comparative analysis of centrosomes and gene expression profiles in cultured normal foreskin fibroblasts, diploid and aneuploid tumor cell lines with and without multipolar mitoses. Most published reports of centrosome analysis in primary tumors and tumor cell lines address the number and morphology of these

structures in interphase nuclei as visualized by immunocytochemistry with antibodies against γ -tubulin or PCNT. In addition to an examination of their presence and abundance in interphase nuclei, we also wanted to determine the manifestations of such aberrations in dividing cells and attempt to make a correlation between these two phases of the cell cycle (Fig. 2). Our analysis included a categorization of interphase and metaphase cells into three distinct classes. Those we labeled as Type 2 and Type 3 corresponded to cells with an increase in centrosome number. According to Theodore Boveri, such cells might be expected to undergo aberrant chromosome segregation. This is in fact what we observed in the pancreatic cell lines, p53HCT116 and *Trp53*–/– MEFs. Whether the resulting daughter cells would be viable is an issue that can only truly be addressed by identifying the aberrant cells and following them through cell division.

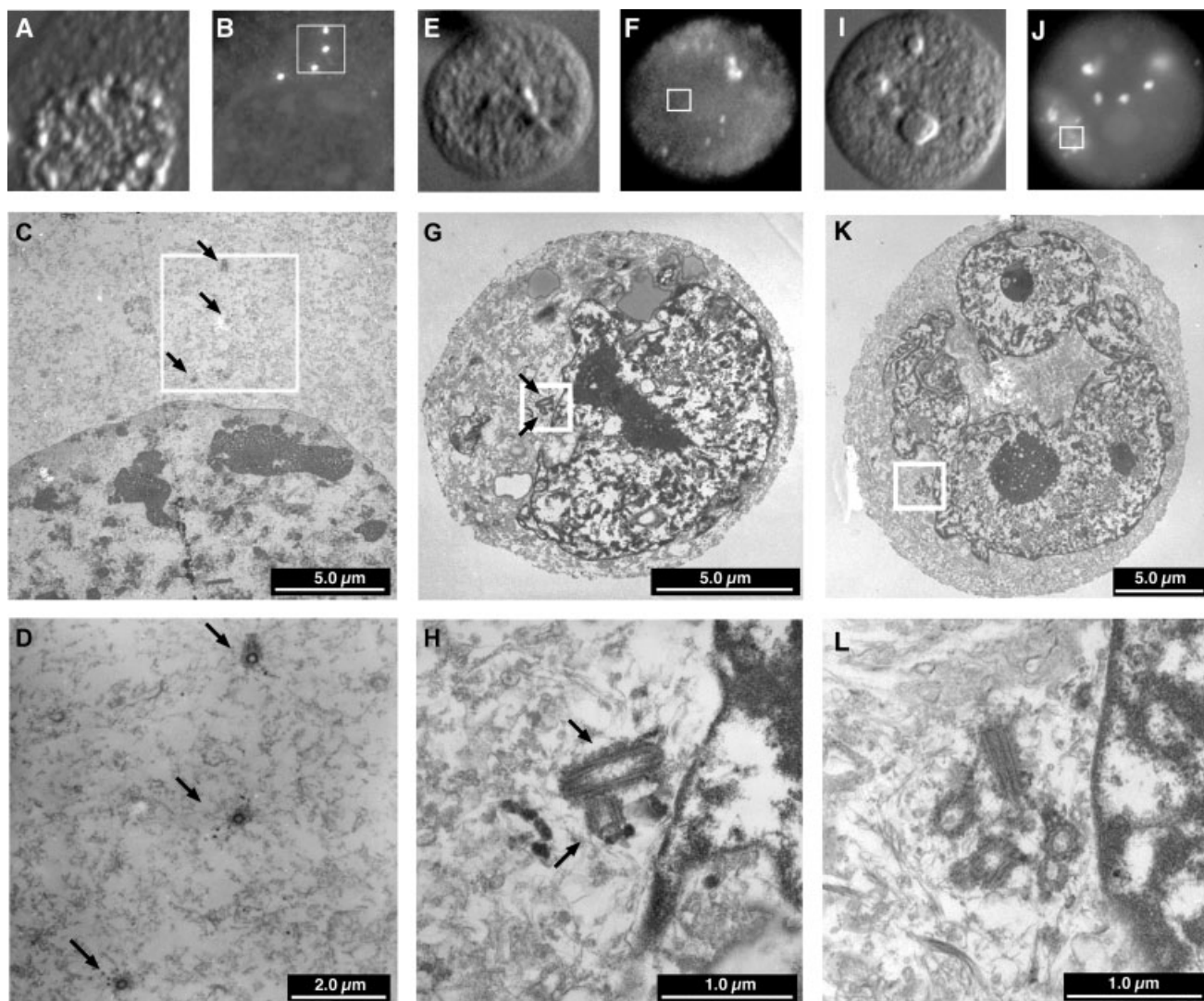


Fig. 6. Immunocytochemistry-electron microscopy (ICC-EM), differential interference contrast (DIC) (A, E, I) and immunofluorescence detection of γ -tubulin (B, F, J) was followed by preparation of serial sections for EM and relocation of the cells with the aid of gridded coverslips. In *Trp53*-deficient MEFs (A–D) and the cell line p53HCT116 (data not shown), every pair of centrioles corresponded to a γ -tubulin structure.

Aneuploid colorectal cells containing multiple γ -tubulin structures usually contained one or two correctly oriented centriole pairs (E–H). Very rarely, however, a cell was observed which contained a cluster of centrioles (I–L), but in association with only one of the many γ -tubulin structures, the others being devoid of centrioles.

The situation, however, was quite different in the CRC cancer cell lines. Defects in DNA mismatch repair pathway (MMR $^{--}$) results in the accumulation of point mutations or small lesions throughout the genome, eventually occurring in tumor suppressor genes or oncogenes. Such genomic alteration abrogates the need for changes in chromosome copy number during tumorigenesis [Lengauer et al., 1998]. Consistent with this mechanism of mutagenesis, we found that these cells contain normal numbers of centrosomes, all of uniform size, shape and protein composition as determined by immunocytochemistry (ICC) against multiple centrosome-associated structural proteins and kinases. Their capacity to nucleate

α -tubulin containing microtubules was similar to control fibroblast cells [Ghadimi et al., 2000] and each centrosome was found to contain two perpendicularly oriented centrioles.

The loss of TP53 function can induce true centrosome amplification in otherwise wildtype (*Trp53* $^{--/-}$ MEFs) and MMR deficient cells (p53HCT116). The *TP53* deficient diploid CRC cell line DLD1, which contains only one to two normal centrosomes, provides evidence that there may be other factors that can counteract this predisposition. Our observations in the p53HCT116 cell line suggest that although TP53 loss can induce the amplification of functional centrosomes and multipolar mitoses in

TABLE II. Differential expression of genes associated with centromeres, centrosomes or spindles

Gene name	Map position	DvM ^a linear ratio	DvM ^a <i>P</i> -value	AvM ^b linear ratio	AvM ^b <i>P</i> -value	AvD ^c linear ratio	AvD ^c <i>P</i> -value	TvM ^d Linear Ratio	TvM ^d <i>P</i> -value	Description
ACTR1A	chr10:104229479-104229420	0.539647305	0.018696017	0.550153772	0.0010171	1.019469136	0.929200173	0.549205278	0.008497794	Homo sapiens ARPI actin-related protein 1 homolog A, centractin alpha (yeast) (ACTR1A), mRNA [NM_005736]
ACTR1A	chr10:104230605-104230546	1.04608995	0.818342947	0.648466369	0.008279034	0.61989542	0.042939928	0.699012881	0.00666194	Homo sapiens ARPI actin-related protein 1 homolog A, centractin alpha (yeast) (ACTR1A), mRNA [NM_005736]
ACTR1A	chr10:104235454-10425395	1.22501463	0.414176537	0.895646251	0.558158895	0.731131065	0.191056088	0.583951097	0.024949017	Homo sapiens ARPI actin-related protein 1 homolog A, centractin alpha (yeast) (ACTR1A), mRNA [NM_005736]
ACTR1B	chr2:97731657-97731598	0.6595558652	0.038408023	0.843711821	0.311689899	1.279206661	0.173222468	0.783190459	0.350625827	Homo sapiens ARPI actin-related protein 1 homolog B, centractin beta (yeast) (ACTR1B), mRNA [NM_005735]
ASPM	chr1:193785170-193785111	10.77544985	4.44757E-06	7.890656212	0.000300598	0.732280909	0.459948772	8.31922161	3.8004E-06	Homo sapiens asp (abnormal spindle)-like, microcephaly associated (Drosophila) (ASPM), mRNA [NM_018136]
ASPM	chr1:193844840-193844781	4.633452771	1.78125E-05	2.596709011	0.019904575	0.560426347	0.131647348	5.120339502	0.000480597	Homo sapiens asp (abnormal spindle)-like, microcephaly associated (Drosophila) (ASPM), mRNA [NM_018136]
AURKA	chr20:54378586-54378527	5.033885486	0.000217951	5.096766692	2.44615E-05	1.012491585	0.963262042	8.378408936	1.93798E-09	Homo sapiens aurora kinase A (AURKA), transcript variant 1, mRNA [NM_198433]
AURKAPI	chr1:1349349-1349193	0.875588444	0.432692593	0.892538657	0.491899499	1.019358654	0.889299865	1.344257482	0.19504244	Homo sapiens aurora kinase A interacting protein 1 (AURKAPI), mRNA [NM_017900]
AURKB	chr17:8051642-8051380	7.872273192	0.000490426	5.595317117	0.000234224	0.710762569	0.39966704	5.433402537	4.42256 E-05	Homo sapiens aurora kinase B (AURKB), mRNA [NM_004217]
AURKC	chr19:62435754-62435813	1.21624842	0.57975991	0.912809485	0.542426431	0.75051237	0.449794723	0.19721149	0.08925087	Homo sapiens aurora kinase C (AURKC), transcript variant 1, mRNA [NM_001015878]
CCDC5	chr18:4:1957282-41958798	2.693528404	0.001496512	2.034856415	0.018498786	0.75546128	0.264585612	0.978815227	0.897631526	Homo sapiens coiled-coil domain containing 5 (spindle associated) (CCDC5), mRNA [NM_138443]
CENPA	chr2:26028565-26928624	14.66658432	2.16592 E-05	11.34106026	8.24114E-05	0.77325845	0.526011482	9.892367239	1.58309E-06	Homo sapiens centromere protein A (CENPA), transcript variant 1, mRNA [NM_001809]

TABLE II. *Continued*

Gene name	Map position	D _v M ^a Linear ratio	D _v M ^a <i>P</i> -value	AvM ^b linear ratio	AvM ^b <i>P</i> -value	AvD ^c linear ratio	AvD ^c <i>P</i> -value	TvM ^d Linear Ratio	TvM ^d <i>P</i> -value	Description
CENPB	chr20:3713453-3713394	0.760030198	0.159655839	1.180472313	0.266016213	1.553191328	0.046935865	0.5537266	0.013168675	Homo sapiens centromere protein B, 80kDa (CENPB), mRNA [NM_001810]
CENPB	chr20:3715043-3714984	1.160296316	0.363689859	1.185731237	0.340074488	1.021921057	0.845679736	0.73662732	0.001802347	Homo sapiens centromere protein B, 80kDa (CENPB), mRNA [NM_001810]
CENPC1	chr4:68169448-68169389	1.160612838	0.405485687	1.059114704	0.684977297	0.912547811	0.624082623	1.118880269	0.372545452	Homo sapiens centromere protein C 1 (CENPC1), mRNA [NM_001812]
CENPC1	chr4:68188382-68187437	1.006709055	0.934194201	0.876358785	0.358993464	0.870518429	0.332645481	0.851713879	0.289385268	Homo sapiens centromere protein C 1 (CENPC1), mRNA [NM_001812]
CENPE	chr4:104385002-104384943	5.080925974	3.94403 <i>E-06</i>	3.963894178	0.001133087	0.780151925	0.449791506	5.788419262	4.83071 <i>E-07</i>	Homo sapiens centromere protein E, 312kDa (CENPE), mRNA [NM_001813]
CENPF	chr1:211214634-211214693	13.31623126	6.81039 <i>E-06</i>	8.593518485	1.4088 <i>E-05</i>	0.645341638	0.139738593	9.487805522	0.000145524	Homo sapiens centromere protein F, 350/400ka (mitosin) (CENPF), mRNA [NM_016343]
CENPF	chr1:211225703-211225762	15.29546784	1.87815 <i>E-07</i>	8.370579827	0.00026139	0.547258829	0.147519816	10.40332935	1.61432 <i>E-06</i>	Homo sapiens centromere protein F, 350/400ka (mitosin) (CENPF), mRNA [NM_016343]
CENPH	chr5:68541405-68541464	9.107266658	0.000127541	7.245875049	9.04981 <i>E-05</i>	0.79561468	0.503731509	6.864131023	0.001168224	Homo sapiens centromere protein H (CENPH), mRNA [NM_022909]
CENPI	chrX:100193585-100201853	4.931762582	0.009120648	6.641217038	1.89721 <i>E-05</i>	1.346621401	0.492460004	15.96776733	0.022712509	Homo sapiens centromere protein I (CENPI), mRNA [NM_006733]
CENPI	chrX:100222701-100224023	5.244225042	0.002512297	5.004508063	0.002597057	0.954289342	0.893063222	12.55296847	0.042236629	Homo sapiens centromere protein I (CENPI), mRNA [NM_006733]
CENPJ	chr13:24355465-24355406	1.922398211	0.015693791	2.160038313	0.02897501	1.123616481	0.722112884	3.433376648	0.001048035	Homo sapiens centromere protein J (CENPJ), mRNA [NM_018451]
CENPJ	chr13:24361516-24361457	2.375437864	0.009754441	2.66206312	0.008230167	1.120662073	0.659930266	2.450784398	0.043428847	Homo sapiens centromere protein J (CENPJ), mRNA [NM_018451]
CENPK	chr5:64849628-64849569	13.37245646	0.028684671	14.21561885	0.017558405	1.063052169	0.871131403	24.60140419	0.02444757	Homo sapiens centromere protein K (CENPK), mRNA [NM_022145]
CENPL	chr1:170503839-170503780	8.302882521	3.66673 <i>E-05</i>	7.379893166	3.666157 <i>E-05</i>	0.888725469	0.704008813	10.18527728	0.026056405	Homo sapiens centromere protein L (CENPL), mRNA [NM_033319]
CENPM	chr22:40666456-40665789	5.553492008	2.62399 <i>E-07</i>	3.998953137	0.000247492	0.72007903	0.223876047	8.952540978	6.72703 <i>E-06</i>	Homo sapiens centromere protein M (CENPM), transcript variant 2, mRNA [NM_001002876]
CENPN	chr16:79598381-79603092	8.210107056	1.78164 <i>E-05</i>	6.192759908	5.47473 <i>E-05</i>	0.754284916	0.361160034	5.703264764	1.02245 <i>E-09</i>	Homo sapiens centromere protein N (CENPN), mRNA [NM_018451]
CENPN	chr16:79611372-79613909	5.821282605	3.28212 <i>E-05</i>	4.440301964	0.000330328	0.762770383	0.379305925	6.851514614	4.41852 <i>E-12</i>	Homo sapiens centromere protein N (CENPN), mRNA [NM_018455]
CENPO	chr2:24952223-2495282	9.686741435	3.2314 <i>E-08</i>	5.299169032	8.30294 <i>E-06</i>	0.547053833	0.017438259	6.06202778	1.69889 <i>E-07</i>	Homo sapiens centromere protein O (CENPO), mRNA [NM_024322]

TABLE II. *Continued*

Gene name	Map position	DvM ^a linear ratio	DvM ^a <i>P</i> -value	AvM ^b linear ratio	AvM ^b <i>P</i> -value	AvD ^c linear ratio	AvD ^c <i>P</i> -value	TvM ^d Linear Ratio	TvM ^d <i>P</i> -value	Description
CENPP	chr9:92455060-92455119	2.88776894	0.000365082	2.467694847	0.005898249	0.854533343	0.581288593	3.776965241	3.8881 <i>E-05</i>	Homo sapiens centromere protein P (CENPP), mRNA [NM_001012267]
CENPQ	chr16:49564899-49564958	2.889926614	0.023577043	2.512399172	0.037472542	0.86936435	0.474572539	1.725225203	0.154183717	Homo sapiens centromere protein Q (CENPQ), mRNA [NM_018132]
CENPT	chr16:66420143-66420084	1.022674924	0.788129804	1.175371187	0.304488725	1.149310655	0.321525946	1.824092922	0.017936524	Homo sapiens centromere protein T (CENPT), mRNA [NM_025082]
CENPT	chr16:66421431-66421372	0.473186734	0.002043084	0.434525475	0.000711106	0.918295979	0.587202789	1.368268765	0.259911193	Homo sapiens centromere protein T (CENPT), mRNA [NM_025082]
CEP110	chr9:120938376-120940257	1.903514736	0.030865732	1.093647861	0.746872002	0.574541316	0.087998296	1.285331062	0.235830586	Homo sapiens centrosomal protein 110kDa (CEP110), mRNA [NM_007018]
CEP110	chr9:121015240-121015299	2.125447106	0.002437274	2.277011447	0.005969369	1.071309392	0.792661283	1.399054603	0.201796018	Homo sapiens centrosomal protein 110kDa (CEP110), mRNA [NM_007018]
CEP135	chr4:56740039-56740098	1.99879018	0.007840708	1.465343529	0.083959271	0.733115233	0.174405033	1.272069603	0.486322049	Homo sapiens centrosomal protein 135kDa (CEP135), mRNA [NM_025009]
CEP152	chr15:46818050-46817991	6.365304608	0.001010772	3.701976961	0.000342989	0.581586772	0.158150536	4.651734824	0.000154524	Homo sapiens centrosomal protein 152kDa (CEP152), mRNA [NM_014985]
CEP152	chr15:46835606-46835547	2.86387685	0.001660254	1.4418171446	0.085179057	0.503468383	0.01677613	3.16611472	0.000112429	Homo sapiens centrosomal protein 152kDa (CEP152), mRNA [NM_014985]
CEP152	chr15:46876919-46876860	5.763911938	0.002469072	3.48895092	0.004439811	0.605309546	0.194190182	9.412200382	0.057854157	Homo sapiens centrosomal protein 152kDa (CEP152), mRNA [NM_014985]
CEP164	chr11:16787812-116788025	1.777902045	0.014046333	1.800247354	5.80363 <i>E-05</i>	1.012568357	0.943495956	1.475793024	0.020343957	Homo sapiens centrosomal protein 164kDa (CEP164), mRNA [NM_014956]
CEP164	chr11:16788900-116788959	1.498076302	0.024992294	1.65791545	0.003670385	1.106747061	0.503469266	2.492997648	0.001292073	Homo sapiens centrosomal protein 164kDa (CEP164), mRNA [NM_014956]
CEP170	chr1:239615116-239615057	1.421950437	0.317851909	1.161020047	0.687824677	0.816498253	0.526860729	0.71943127	0.407049036	Homo sapiens centrosomal protein 170kDa (CEP170), transcript variant alpha, mRNA [NM_014812]
CEP170	chr1:239615751-239615693	1.238051333	0.482605789	1.440667912	0.222881189	1.163657656	0.530740462	0.922267283	0.861385217	Homo sapiens centrosomal protein 170kDa (CEP170), transcript variant alpha, mRNA [NM_014812]
CEP170	chr1:239615909-239615850	2.671694398	0.018583254	2.069706728	0.060888338	0.774679443	0.355862574	1.05375875	0.951032725	Homo sapiens centrosomal protein 170kDa (CEP170), transcript variant alpha, mRNA [NM_014812]

TABLE II. *Continued*

Gene name	Map position	D _v M ^a linear ratio	D _v M ^a <i>P</i> -value	A _v M ^b linear ratio	A _v M ^b <i>P</i> -value	A _v D ^c linear ratio	A _v D ^c <i>P</i> -value	T _v M ^d Linear Ratio	T _v M ^d <i>P</i> -value	Description
CEP192	chr18:13114695-13114754	2.388743046	0.008390604	1.985524549	0.002282799	0.831200556	0.446086642	1.84448137	0.021286845	Homo sapiens centrosomal protein 192kDa (CEP192), transcript variant 2, mRNA [NM_018069]
CEP250	chr20:33518300-33518590	1.644863155	0.039344698	1.832296492	0.002207924	1.113950718	0.635026044	2.367640393	0.00048323	Homo sapiens centrosomal protein 250kDa (CEP250), transcript variant 1, mRNA [NM_007186]
CEP250	chr20:33562995-33563054	1.388370642	0.051002882	1.424900352	0.058394494	1.026311209	0.881085598	3.035913597	0.000564547	Homo sapiens centrosomal protein 250kDa (CEP250), transcript variant 1, mRNA [NM_007186]
CEP27	chr15:40640846-40643251	4.880353597	6.12646 E-06	3.564077959	3.7139 E-06	0.730290928	0.021523266	2.216863674	3.22586 E-06	Homo sapiens centrosomal protein 27kDa (CEP27), mRNA [NM_018097]
CEP290	chr12:86945362-86945303	2.482050252	0.001844159	1.719359227	0.005551278	0.692717331	0.077176961	1.560414439	0.022656252	Homo sapiens centrosomal protein 290kDa (CEP290), mRNA [NM_025114]
CEP290	chr12:86990086-86990027	2.13299736	0.046439019	1.240500022	0.228630892	0.581575976	0.114019801	1.161237974	0.40539539	Homo sapiens centrosomal protein 290kDa (CEP290), mRNA [NM_025114]
CEP290	chr12:87007554-87007495	1.775771373	0.014549972	1.146451569	0.305207578	0.645607642	0.03979151	1.335703384	0.15972627	Homo sapiens centrosomal protein 290kDa (CEP290), mRNA [NM_025114]
CEP350	chr1:176813814-176813873	0.602432222	0.031185402	0.750128266	0.121492348	1.245166242	0.180520516	0.793239701	0.36640114	Homo sapiens centrosomal protein 350kDa (CEP350), mRNA [NM_014810]
CEP55	chr10:95278744-95278803	15.24264981	5.10241 E-06	9.267558577	0.000134993	0.608001803	0.250198277	9.489143833	4.0384 E-09	Homo sapiens centrosomal protein 55kDa (CEP55), mRNA [NM_018131]
CEP57	chr11:95195182-95195241	3.754974244	0.002205218	3.483850989	0.002501611	0.927796241	0.735439741	0.966981407	0.907651468	Homo sapiens centrosomal protein 57kDa, mRNA (cDNA clone MGC:47657 IMAGE:5415088), complete cds. [BC039711]
CEP57	chr11:95204441-95204500	1.336414985	0.151671351	1.526372732	0.002837711	1.142139792	0.483345057	0.963759505	0.794560563	Homo sapiens centrosomal protein 57kDa (CEP57), mRNA [NM_014679]
CEP63	chr3:135708732-135708791	0.760254948	0.250754967	0.687965536	0.020752188	0.90491425	0.657505573	0.917784601	0.510706156	Homo sapiens centrosomal protein 63kDa (CEP63), transcript variant 1, mRNA [NM_025180]
CEP63	chr3:135751687-135751746	0.78571475	0.230862624	0.901251733	0.48501956	1.147046983	0.443665717	0.716637178	0.035471074	Homo sapiens centrosomal protein 63kDa (CEP63), transcript variant 1, mRNA [NM_025180]
CEP68	chr2:65211270-65211329	1.428281542	0.009524892	1.155090073	0.468734657	0.808727159	0.281613256	1.297912414	0.389265625	Homo sapiens centrosomal protein 68kDa (CEP68), mRNA [NM_015147]
CEP70	chr3:139702062-139702003	1.324438542	0.184212325	0.849397439	0.488493314	0.641326428	0.100758416	0.63599027	0.012980306	Homo sapiens centrosomal protein 70kDa (CEP70), mRNA [NM_024491]

TABLE II. *Continued*

Gene name	Map position	DvM ^a linear ratio	DvM ^a <i>P</i> -value	AvM ^b linear ratio	AvM ^b <i>P</i> -value	AvD ^c linear ratio	AvD ^c <i>P</i> -value	TvM ^d Linear Ratio	TvM ^d <i>P</i> -value	Description
CEP70	chr3:139771888-139738859	1.430083122	0.254485206	0.963065396	0.869853138	0.67343316	0.234549471	0.635790888	0.025818277	Homo sapiens centrosomal protein 70kDa (CEP70), mRNA [NM_024491]
CEP72	chr5:706323-706382	8.032716663	0.000101596	8.289461078	1.92135 <i>E</i> -07	1.031962339	0.903396806	10.25139941	3.41397 <i>E</i> -08	Homo sapiens centrosomal protein 72kDa (CEP72), mRNA [NM_018140]
CEP76	chr18:12664543-12663452	4.339251362	0.00224282	3.798982475	2.62339 <i>E</i> -05	0.875492604	0.675830323	1.252748527	0.154761209	Homo sapiens centrosomal protein 76kDa (CEP76), mRNA [NM_024899]
CEP78	chr9:78115584-78115643	4.846245748	0.001425178	2.206902652	0.033235032	0.455383975	0.003817319	2.382707804	0.013801704	Homo sapiens centrosomal protein 78kDa, mRNA (cDNA clone IMAGE:61194709), complete cds. [BC091515]
CETN1	chr18:571466-571525	n/a	n/a	n/a	n/a	n/a	1.161456339	n/a	n/a	Homo sapiens centrin, EF-hand protein, 1 (CETN1), mRNA [NM_004066]
CETN2	chrX:151666808-151666749	0.501943496	0.008099263	1.119875238	0.58234511	2.231078295	0.000104316	1.049006507	0.776719386	Homo sapiens centrin, EF-hand protein, 2 (CETN2), mRNA [NM_004344]
CETN3	chr5:89730993-89730934	3.092503925	0.001160663	1.861321435	0.019098216	0.601881673	0.030064776	1.178904169	0.404238164	Homo sapiens centrin, EF-hand protein, 3 (CDC31 homolog, yeast) (CETN3), mRNA [NM_004365]
CKAP1	chr19:41308258-41308461	1.051873377	0.786514087	0.852142898	0.401057334	0.810119276	0.285933167	1.138465716	0.531417602	Homo sapiens cytoskeleton associated protein 1 (CKAP1), mRNA [NM_001281]
CKAP2	chr13:51933864-51933923	11.22581574	1.46171 <i>E</i> -05	10.48840925	6.78574 <i>E</i> -06	0.934311545	0.831813717	29.80248539	n/a	Homo sapiens cytoskeleton associated protein 2 (CKAP2), mRNA [NM_018204]
CKAP2	chr13:51948395-51948454	10.54431952	0.000178184	7.947936999	4.45488 <i>E</i> -05	0.75376481	0.329337053	6.054208437	0.000299478	Homo sapiens cytoskeleton associated protein 2 (CKAP2), mRNA [NM_018204]
CKAP2L	chr2:113212048-113211989	16.97870637	1.58193 <i>E</i> -06	12.85249895	3.03004 <i>E</i> -05	0.756977515	0.493586254	12.84382198	3.24863 <i>E</i> -11	Homo sapiens cytoskeleton associated protein 2-like (CKAP2L), mRNA [NM_152515]
CKAP4	chr12:105134998-105134939	1.192424072	0.539105116	1.693828458	0.128720564	1.420491667	0.399268907	1.465653433	0.067533936	Homo sapiens cytoskeleton-associated protein 4 (CKAP4), mRNA [NM_006825]
CKAP5	chr11:46722100-46722041	2.263895189	1.42451 <i>E</i> -05	2.165037942	3.07016 <i>E</i> -06	0.956333116	0.678260735	2.61956866	3.08061 <i>E</i> -05	Homo sapiens cytoskeleton associated protein 5 (CKAP5), transcript variant 1, mRNA [NM_00108938]
CKAP5	chr11:46728512-46728453	3.593201945	0.000428454	3.563956667	1.31413 <i>E</i> -07	0.991860942	0.962482903	2.415876152	0.007136492	Homo sapiens cytoskeleton associated protein 5 (CKAP5), transcript variant 1, mRNA [NM_00108938]

TABLE II. Continued

Gene name	Map position	D _v M ^a linear ratio	D _v M ^a P- value	A _v M ^b linear ratio	A _v M ^b P-value	A _v D ^c linear ratio	A _v D ^c P-value	T _v M ^d Linear Ratio	T _v M ^d P-value	Description
CNTROB	chr17:7791983-7792219	1.380090445	0.147794125	1.188513785	0.194224222	0.861185431	0.484869864	1.074462385	0.599837685	Homo sapiens centrobin, centrosomal BRCA2 interacting protein (CNTROB), transcript variant 1, mRNA [NM_053051]
CNTROB	chr17:7793143-7793429	1.333007534	0.017272461	1.060273067	0.710207071	0.795399156	0.159160311	1.444629856	0.013689337	Homo sapiens centrobin, centrosomal BRCA2 interacting protein (CNTROB), transcript variant 1, mRNA [NM_053051]
CSPP1	chr8:68170424-68170483	1.85414209	9.72806 E-05	1.250798595	0.041178529	0.674596948	0.0004908/4	1.822661654	3.73583 E-06	Homo sapiens centrosome and spindle pole associated protein 1 (CSPP1), mRNA [NM_024790]
CSPP1	chr8:68206803-68206862	1.355004111	0.054170198	0.688085399	0.001863954	0.507810562	0.001200116	1.779930558	0.006905074	Homo sapiens centrosome and spindle pole associated protein 1 (CSPP1), mRNA [NM_024790]
CSPP1	chr8:68270186-68270245	2.714129926	0.00047888	1.768188301	0.008985281	0.651475187	0.009680708	2.553363272	0.000371821	Homo sapiens centrosome and spindle pole associated protein 1 (CSPP1), mRNA [NM_024790]
ESPL1	chr12:51950737-51950796	n/a	n/a	n/a	n/a	0.841553567	0.842833898	1.852540929	n/a	Homo sapiens extra spindle poles like 1 (<i>S. cerevisiae</i>) (ESPL1), mRNA [NM_012291]
ESPL1	chr12:51973015-51973376	3.254837903	0.041239758	1.932918036	0.20586329	0.59386	0.075112613	4.05140709	0.082693087	Homo sapiens extra spindle poles like 1 (<i>S. cerevisiae</i>) (ESPL1), mRNA [NM_012291]
GCET2	chr3:113328551-113325307	2.389227262	0.294056971	0.551039068	0.307032374	0.230634849	0.133085603	0.161110006	n/a	Homo sapiens germinal center expressed transcript 2 (GCET2), transcript variant 2, mRNA [NM_001008756]
INCENP	chr11:61676318-61676377	3.697943337	1.33517 E-05	2.832056481	0.000569571	0.76584637	0.235018719	4.941445961	3.98785 E-10	Homo sapiens inner centromere protein antigens 135/155kDa (INCENP), transcript variant 2, mRNA [NM_020238]
LOC645904	chr22:22127982-22128041	0.441940165	0.282159047	2.182286412	0.320371214	4.937968039	0.058693174	0.248154139	0.023823843	PREDICTED: Homo sapiens similar to Mitotic spindle assembly checkpoint protein MAD1 (Mitotic arrest deficient-like protein 1) (MAD1-like 1)
NUSAP1	chr15:39455237-39455296	10.73924377	2.41311 E-06	6.846925166	5.84109 E-05	0.637561202	0.181184705	6.16505977	1.39808 E-08	(Mitotic checkpoint MAD1 protein-homolog) (HsMAD1) (hMAD1) (Tax-binding protein 181) (LOC645904), mRNA [XM_928876]
NUSAP1	chr15:39455237-39455296	10.73924377	2.41311 E-06	6.846925166	5.84109 E-05	0.637561202	0.181184705	6.16505977	1.39808 E-08	Homo sapiens nucleolar and spindle associated protein 1 (NUSAP1), transcript variant 1, mRNA [NM_016359]

TABLE II. Continued

Gene name	Map position	DvM ^a linear ratio	DvM ^a <i>P</i> -value	AvM ^b linear ratio	AvM ^b <i>F</i> -value	AvD ^c linear ratio	AvD ^c <i>P</i> -value	TvM ^d Linear Ratio	TvM ^d <i>P</i> -value	Description
PCNT	chr21:46607847- 46607906	1.995536761	0.003603067	1.147115076	0.438068366	0.574840363	0.011131725	1.599365964	0.034052472	Homo sapiens pericentrin (kendrin) (PCNT), mRNA [NM_006031]
PCNT	chr21:46689818- 46689877	2.13151517	0.009587076	1.535881154	0.029989851	0.720558397	0.164662802	1.74927465	0.025662446	Homo sapiens pericentrin (kendrin) (PCNT), mRNA [NM_006031]
PLK1	chr16:23608471- 23608713	3.265872419	0.005250644	3.208935199	0.00025727	0.982566	0.956385248	7.3375786	0.000767782	Homo sapiens polo-like kinase 1 (Drosophila) (PLK1), mRNA [NM_005030]
PLK1	chr16:23609129- 23609188	4.787465478	0.000781001	4.08903615	0.000354447	0.854112927	0.630617439	7.443472158	1.32082 E-10	Homo sapiens polo-like kinase 1 (Drosophila) (PLK1), mRNA [NM_005030]
PLK2	chr5:57783809- 57785750	3.488306828	0.0244796	1.521062725	0.117594995	0.436046139	0.09118439	1.02254131	0.887469567	Homo sapiens polo-like kinase 2 (Drosophila) (PLK2), mRNA [NM_006622]
PLK3	chr1:44940687- 44940747	2.435368737	0.109707642	1.201460306	0.558596682	0.49333815	0.195117292	1.620874084	0.069446961	Homo sapiens polo-like kinase 3 (Drosophila) (PLK3), mRNA [NM_004073]
PLK4	chr4:129164616- 129164675	n/a	n/a	n/a	n/a	0.895450209	0.60614004	5.199779736	n/a	Homo sapiens polo-like kinase 4 (Drosophila) (PLK4), mRNA [NM_014264]
PLK4	chr4:129173787- 129173846	11.32166634	1.91662 E-05	8.767602137	3.42365 E-05	0.774409161	0.478940104	15.54431987	0.046930589	Homo sapiens polo-like kinase 4 (Drosophila) (PLK4), mRNA [NM_014264]
SASS6	chr1:100261677- 100261618	3.04994683	0.001368359	2.739787511	0.002069993	0.898306647	0.609683684	3.516256585	0.014796998	Homo sapiens spindle assembly 6 homolog (C. elegans) (SASS6), mRNA [NM_194292]
SERF1B	chr5:69356972- 69357031	1.589652955	0.029834219	1.239638287	0.352283979	0.77981693	0.241576165	1.547922151	0.076344482	Homo sapiens small EDRK-rich factor 1B (centromeric) (SERF1B), mRNA [NM_022978]
SERF1B	chr5:69374401- 69374460	1.023819803	0.875568098	1.23633913	0.280545039	1.207628441	0.318605991	1.296395013	0.212592082	Homo sapiens small EDRK-rich factor 1B (centromeric) (SERF1B), mRNA [NM_022978]
SFI1	chr22:30337566- 30338661	1.145225859	0.606425131	0.765941736	0.25362742	0.66881282	0.062296319	1.616553871	0.182497052	Homo sapiens Sfi1 homolog, spindle assembly associated (yeast) (SFI1), transcript variant 1, mRNA [NM_001007467]
SFI1	chr22:30338984- 30339043	0.969564121	0.927280494	0.667412121	0.167391802	0.688363056	0.179544473	1.708216391	0.109655104	Homo sapiens Sfi1 homolog, spindle assembly associated (yeast) (SFI1), transcript variant 1, mRNA [NM_001007467]
SMN2	chr5:69398703- 69398921	2.137039469	0.030982119	1.90124909	0.023116142	0.88966494	0.699783579	0.783099838	0.422866214	Homo sapiens survival of motor neuron 2, centromeric (SMN2), transcript variant c, mRNA [NM_022877]

TABLE II. *Continued*

Gene name	Map position	DvM ^a linear ratio	DvM ^a <i>P</i> -value	AvM ^b linear ratio	AvM ^b <i>P</i> -value	AvD ^c linear ratio	AvD ^c <i>P</i> -value	TvM ^d Linear Ratio	TvM ^d <i>P</i> -value	Description
SPBC24	chr19:11118053-11117994	2.986090864	0.000543131	2.931432497	0.00578461	0.981695678	0.951721418	5.353491369	0.000107404	Homo sapiens spindle pole body component 24 homolog (S. cerevisiae) (SPBC24), mRNA [NM_182513]
SPBC25	chr2:169553522-169553463	16.74630849	7.27785 <i>E-06</i>	9.383383693	0.0000302853	0.560325501	0.227108378	11.85578736	3.16569 <i>E-07</i>	Homo sapiens spindle pole body component 25 homolog (S. cerevisiae) (SPBC25), mRNA [NM_020675]
SYCE1	chr10:135259492-13559189	1.184337701	0.068071939	1.286719934	n/a	1.086446824	n/a	0.199583466	0.10467662	Homo sapiens synaptoneuronal complex central element protein 1 (SYCE1), transcript variant 2, mRNA [NM_201564]
THC2343415 chr4:124009351-124009292		2.143457766	0.043669847	1.49395673	0.206816648	0.696984449	0.332591864	0.574745619	n/a	Q5SUE1 (Q5SUE1) Centrin 4, partial (52%) [THC2343415]
76P	chr15:414843980-414844039	5.950048853	0.000136909	4.643172054	0.000223346	0.780358644	0.147011559	1.881091083	0.003462753	Homo sapiens gamma tubulin ring complex protein (76p gene) (76P), mRNA [NM_014444]
AA780798	chr6:030799960-030799901	1.978180711	0.002137747	1.591348	0.039743857	0.804450242	0.302976729	1.600971506	0.036356944	ag14d07.s1 Gessler Wilms tumor Homo sapiens cDNA clone IMAGE:1070317 3' similar to gb:J00314_ma2_TUBULIN_BETA-1_CHAIN (HUMAN); mRNA sequence [AA780798]
A1028577	chr2:132074237-132074178	0.679517636	0.181584774	1.1115795872	0.570128513	1.642041079	0.100541347	0.854957638	0.834643704	Soares_testis_NHT Homo sapiens cDNA clone IMAGE:1645605 3' similar to gb:K00558_TUBULIN_ALPHA-1_CHAIN (HUMAN); mRNA sequence [A1028577]
A1608782	chr12:47808298-47808357	1.255935486	0.237944754	1.18596674	0.435074234	0.944289538	0.806340361	1.459355627	0.130521468	NCL_CGAP_HN6 Homo sapiens cDNA clone IMAGE:2267384 3' similar to gb:K00558_TUBULIN_ALPHA-1_CHAIN (HUMAN); mRNA sequence [A1608782]
AI911586	chr10:104492950-104492891	n/a	n/a	n/a	n/a	0.720982417	0.283031701	18.86056627	n/a	ty73h01.x1 NCL_CGAP_Kid11 Homo sapiens cDNA clone IMAGE:2284753 3' similar to SW:TTL_PIG_P38160 TUBULIN-TYROSINE LIGASE; mRNA sequence [A1911586]

TABLE II. *Continued*

Gene name	Map position	DvM ^a linear ratio	DvM ^a <i>P</i> -value	AvM ^b linear ratio	AvM ^b <i>P</i> -value	AvD ^c linear ratio	AvD ^c <i>P</i> -value	TvM ^d Linear Ratio	TvM ^d <i>P</i> -value	Description
AW16845	chr16:88529508- 088529449	1.671060959	0.017452552	1.342976619	0.181410468	0.803667042	0.205957476	1.333594604	0.083987165	xg60e01.x1 NCL_CGAP_Ut4 Homo sapiens cDNA clone IMAGE:2632728 3' similar to gb:X00734_cds1 TUBULIN BETA-5 CHAIN (HUMAN); mRNA sequence [AW16845]
BC014971	chr16:88690155- 88690214	2.789518804	0.093886023	1.070134041	0.908832914	0.383626753	0.171254557	1.767978642	0.192001611	Homo sapiens, Similar to tubulin, beta, 2, clone IMAGE:4873024, mRNA. [BC014971]
H2-ALPHA	chr2:132071974- 132072033	0.969319995	0.888268077	1.088894578	0.72631665	1.123359245	0.584331437	0.854448924	0.495356593	Homo sapiens alpha-tubulin isotype H2-alpha (H2-ALPHA), mRNA [NM_080386]
H2-ALPHA	chr2:132074162- 132074221	1.105076099	0.604403333	0.963805346	0.833609939	0.872161969	0.250552949	0.734974792	0.104123911	Homo sapiens alpha-tubulin isotype H2-alpha (H2-ALPHA), mRNA [NM_080386]
K-ALPHA-1	chr12:47807959- 47807900	0.857443642	0.560459713	1.185047241	0.604422153	1.382070125	0.325594025	1.174717108	0.580060146	Homo sapiens alpha tubulin (K-ALPHA-1), mRNA [NM_006082]
MGC16703	chr22:19688101- 1968042	1.189996746	0.569120291	1.255005399	0.498103922	1.054629269	0.831504271	0.356314526	0.004960059	Homo sapiens alpha tubulin-like (MGC16703), mRNA [NM_145042]
TBCA	chr5:77023014- 77022955	1.628337401	0.015750817	1.207337195	0.333723591	0.741453948	0.188358639	0.971893895	0.869550385	Homo sapiens tubulin-specific chaperone a (TBCA), mRNA [NM_004607]
TBBC	chr6:42820720- 42820661	0.995875905	0.985422176	1.589501306	0.126759341	1.596083707	0.084494378	1.176170582	0.527720869	Homo sapiens tubulin-specific chaperone c (TBCC), mRNA [NM_003192]
TBBC	chr6:42820889- 42820830	1.003613754	0.984482864	1.67612549	0.063421457	1.670090195	0.031748746	1.041677783	0.878930352	Homo sapiens tubulin-specific chaperone c (TBCC), mRNA [NM_003192]
TBCD	chr17:78477601- 78478354	1.488387681	0.214609459	1.723997872	0.019360207	1.158298939	0.627420613	1.226622933	0.495345392	Homo sapiens tubulin-specific chaperone d (TBCD), transcript variant 1, mRNA [NM_005993]
TBCD	chr17:78488452- 78488511	1.399249127	0.175479398	1.213985031	0.173144039	0.86759749	0.56657747	1.748825524	0.007044583	Homo sapiens tubulin-specific chaperone d (TBCD), transcript variant 1, mRNA [NM_005993]
TBCD	chr17:78493800- 78493859	1.19735066	0.409177942	1.044632883	0.775196054	0.872453591	0.565410914	2.334565662	0.0011132949	Homo sapiens tubulin-specific chaperone d (TBCD), transcript variant 1, mRNA [NM_005993]
TBCE	chr1:23:1938185- 231938244	1.70187682	0.008802425	1.923716165	0.000232169	1.130349825	0.468937133	1.674976767	0.003741768	Homo sapiens tubulin-specific chaperone e (TBCE), mRNA [NM_003193]

TABLE II. Continued

Gene name	Map position	D _v M ^a linear ratio	D _v M ^a P-value	A _v M ^b linear ratio	A _v M ^b P-value	A _v D ^c linear ratio	A _v D ^c P-value	T _v M ^d Linear Ratio	T _v M ^d P-value	Description
THC2307581	chr6:003169718-003169777	1.952910606	0.62434615	3.352015778	0.135931051	1.71642049	0.707633847	0.045570054	0.033095821	B25437 tubulin beta-2 chain - mouse (fragment) [Mus musculus], partial (18%)
THC2307600	chr6:40075674-40075734	0.840555216	0.329703812	0.833605185	0.406911044	0.991731619	0.96364418	0.920517101	0.798113018	Q9JJY6 (Q9JJY6) Beta-tubulin (Fragment), partial (46%)
TTBK2	chr15:40825647-40825588	0.775213323	0.265200427	1.243886247	0.349996464	1.604572844	0.024574108	0.710933596	0.31385279	Homo sapiens tau tubulin kinase 2 (TTBK2), mRNA [NM_173500]
TTBK2	chr15:40856649-40856590	2.339489963	0.047526696	2.276855802	0.044370793	0.973227429	0.935856907	0.884497395	0.622843256	Homo sapiens tau tubulin kinase 2 (TTBK2), mRNA [NM_173500]
TTL	chr2:112968040-112968099	6.663981858	0.000240118	3.010395864	0.002774944	0.451741305	0.003176487	1.511421614	0.1010284	Homo sapiens tubulin tyrosine ligase (TTL), mRNA [NM_153712]
TTL	chr2:112976906-112976965	14.4020585	2.891 E-05	5.296386338	4.9465 E-05	0.367752036	0.010429262	3.343359036	0.239889706	Homo sapiens tubulin tyrosine ligase (TTL), mRNA [NM_153712]
TTL	chr2:13002674-113002733	5.408645901	0.000358103	2.956077359	0.005525021	0.546546661	0.044370259	1.848052212	0.001789355	Homo sapiens tubulin tyrosine ligase (TTL), mRNA [NM_153712]
TLLL1	chr22:41772389-41772330	2.455246928	0.004617839	1.608578367	0.082121147	0.655159507	0.044975404	1.001655349	0.995238055	Homo sapiens tubulin tyrosine ligase-like family, member 1 (TLLL1), transcript variant 2, mRNA [NM_001008572]
TLLL10	chr1:1160312-1160371	n/a	n/a	n/a	n/a	1.326906974	n/a	2.978726245	n/a	Homo sapiens tubulin tyrosine ligase-like family, member 10 (TLLL10), mRNA [NM_153254]
TLLL11	chr9:121831419-121831360	0.698405365	0.182417357	0.630991229	0.048646634	0.903474202	0.729798999	0.647220855	0.120318237	Homo sapiens tubulin tyrosine ligase-like family, member 11 (TLLL11), mRNA [NM_194252]
TLLL12	chr22:41887399-41887340	2.138427795	0.0014636	1.858673953	0.00429454	0.869177794	0.386698421	2.855889328	0.000450266	Homo sapiens tubulin tyrosine ligase-like family, member 12 (TLLL12), mRNA [NM_015140]
TLLL2	chr6:167725671-167725730	n/a	n/a	n/a	n/a	n/a	n/a	1.628620287	n/a	Homo sapiens tubulin tyrosine ligase-like family, member 2 (TLLL2), mRNA [NM_031949]
TLLL3	chr3:9843876-9843935	0.344169157	0.001825435	0.292954647	0.000801308	0.851193782	0.304955949	0.485375458	0.008726558	Homo sapiens tubulin tyrosine ligase-like family, member 3, mRNA (cDNA clone IMAGE:3841498), complete cds. [BC009479]
TLLL3	chr3:9851825-9851884	1.065101337	0.676523871	0.774999999	0.101099692	0.727630294	0.071154571	2.437055254	0.000714055	Homo sapiens tubulin tyrosine ligase-like family, member 3, mRNA (cDNA clone IMAGE:3841498), complete cds. [NM_015644]

TABLE II. *Continued*

Gene name	Map position	DvM ^a linear ratio	DvM ^a <i>P</i> -value	AvM ^b linear ratio	AvM ^b <i>P</i> -value	AvD ^c linear ratio	AvD ^c <i>P</i> -value	TvM ^d Linear Ratio	TvM ^d <i>P</i> -value	Description
TTLL3	chr3:9852427-9852486	0.731172239	0.19043441	0.805874282	0.309120618	1.102167505	0.638033707	2.514457619	0.006736965	Homo sapiens tubulin tyrosine ligase-like family, member 3 (TTLL3), transcript variant 2, mRNA [NM_015644]
TTLL4	chr2:219443837-219443896	2.550471097	0.000415031	3.571844465	2.43491 <i>E</i> -05	1.400464592	0.009065142	3.094473776	0.006425222	Homo sapiens tubulin tyrosine ligase-like family, member 4 (TTLL4), mRNA [NM_014640]
TTLL5	chr14:75399792-75399851	1.155370394	0.596550761	1.824202391	0.001201405	1.57888968	0.139034148	2.380077506	9.96478 <i>E</i> -08	Homo sapiens tubulin tyrosine ligase-like family, member 5 (TTLL5), mRNA [NM_015072]
TTLL6	chr17:44195237-44195178	0.43520045	0.150939071	0.822730613	0.77291541	1.90080367	0.235451172	0.342220962	0.299756463	Homo sapiens tubulin tyrosine ligase-like family, member 6 (TTLL6), mRNA [NM_173623]
TTLL6	chr17:44217418-44217359	0.608140153	n/a	0.746786542	n/a	1.22798427	n/a	0.611001865	0.653278394	Homo sapiens tubulin tyrosine ligase-like family, member 6 (TTLL6), mRNA [NM_173623]
TTLL7	chr1:84068058-84060815	1.648672303	0.354687912	0.519839499	0.288668436	0.315307959	0.112306095	0.080480022	3.35687 <i>E</i> -05	Homo sapiens tubulin tyrosine ligase-like family, member 7 (TTLL7), mRNA [NM_024686]
TTLL7	chr1:84081836-84068180	1.310065691	0.611118581	0.964126748	0.964425663	0.735937712	0.727708411	0.027896848	3.02846 <i>E</i> -07	Homo sapiens tubulin tyrosine ligase-like family, member 7 (TTLL7), mRNA [NM_024686]
TUBA1	chr2:219440634-219440575	0.572675993	0.087416476	1.104193813	0.805321055	1.928130087	0.164332075	2.126422654	0.008900223	Homo sapiens tubulin, alpha 1 (testis specific) (TUBA1), mRNA [NM_006000]
TUBA1	chr2:219440711-219940652	0.687745013	0.202200336	1.269904259	0.540851238	1.846475417	0.183063653	1.951896463	0.017287701	Homo sapiens tubulin, alpha 1 (testis specific) (TUBA1), mRNA [NM_006000]
TUBA1	chr2:219940759-219940700	0.750639634	0.102679812	1.081207133	0.734460844	1.440381088	0.137420149	1.152073381	0.54717231	Homo sapiens tubulin, alpha 1 (testis specific) (TUBA1), mRNA [NM_006000]
TUBA1	chr2:219441227-219941168	0.849512285	0.379802777	1.298166666	0.33820833	1.528131717	0.162818869	1.760373391	0.020135594	Homo sapiens tubulin, alpha 1 (testis specific) (TUBA1), mRNA [NM_006000]
TUBA2	chr13:18649197-18649138	1.119600211	0.626472071	1.816294981	0.047888997	1.622271024	0.162113969	2.514239847	0.010244898	Homo sapiens tubulin, alpha 2 (TUBA2), transcript variant 2, mRNA [NM_079836]
TUBA3	chr12:47865739-47865680	0.939133616	0.821975246	1.160677517	0.585287238	1.235902428	0.460677371	0.845469497	0.506095413	Homo sapiens tubulin, alpha 3 (TUBA3), mRNA [NM_006009]
TUBA6	chr12:47949701-47949900	1.13867431	0.670390308	1.458724134	0.175768655	1.281072314	0.425444758	0.896282829	0.679542622	Homo sapiens tubulin, alpha 6 (TUBA6), mRNA [NM_032704]
TUBA6	chr12:47952552-47952611	1.439720094	0.184643278	1.671964313	0.051572976	1.161312063	0.593785586	1.146649828	0.511143061	Homo sapiens tubulin, alpha 6 (TUBA6), mRNA [NM_032704]

TABLE II. Continued

Gene name	Map position	DvM ^a linear ratio	DvM ^a P-value	AvM ^b linear ratio	AvM ^b P-value	AvD ^c linear ratio	AvD ^c P-value	TvM ^d Linear Ratio	TvM ^d P-value	Description
TUBA6	chr12:47953065-47953124	1.096186884	0.659628265	1.364777204	0.187923114	1.245022381	0.426930697	1.263565105	0.298454674	Homo sapiens tubulin, alpha 6 (TUBA6), mRNA [NM_032704]
TUBA6	chr12:47953297-47953356	2.519503536	0.004459479	2.463328773	0.00149327	0.977704035	0.931823772	2.773231793	0.000728057	Homo sapiens tubulin, alpha 6 (TUBA6), mRNA [NM_032704]
TUBA8	chr22:16988374-16988433	1.004108425	0.989047759	0.953525457	0.80109154	0.949623998	0.856962984	1.167233958	0.393680863	Homo sapiens tubulin, alpha 8 (TUBA8), mRNA [NM_018943]
TUBA13	chr10:5425268-5425209	0.204902439	0.255851845	0.994791897	0.996833074	4.834955908	0.030404166	1.092128748	0.947104434	Homo sapiens tubulin, alpha-like 3 (TUBA13), mRNA [NM_024803]
TUBB	chr6:30799847-3079906	1.584278885	0.00566468	1.372285719	0.184164808	0.866189489	0.517774048	1.524299646	0.04644169	Homo sapiens tubulin, beta (TUBB), mRNA [NM_178014]
TUBB	chr6:30799884-3079943	1.492109899	0.079513857	1.244767024	0.453531673	0.834232804	0.493657273	1.234137979	0.376482678	Homo sapiens tubulin, beta (TUBB), mRNA [NM_178014]
TUBB	chr6:30800501-30800560	1.584623411	0.107036108	1.554573084	0.12797646	0.981036297	0.947810448	1.767278199	0.074347725	Homo sapiens tubulin, beta (TUBB), mRNA [NM_178014]
TUBB1	chr20:57033076-57033135	1.283709237	n/a	n/a	n/a	n/a	n/a	0.560774764	n/a	Homo sapiens tubulin, beta 1 (TUBB1), mRNA [NM_030773]
TUBB1	chr20:57034639-57034698	n/a	n/a	n/a	n/a	0.623141934	n/a	1.150873305	n/a	Homo sapiens tubulin, beta 1 (TUBB1), mRNA [NM_030773]
TUBB2A	chr6:3099093-3099034	0.515399738	0.128243869	0.223915793	0.001080418	0.434450731	0.106193622	0.225151386	0.000305294	Homo sapiens tubulin, beta 2A (TUBB2A), mRNA [NM_001069]
TUBB2A	chr6:3099458-3099399	0.953497535	0.865848881	0.569640111	0.099851658	0.597421692	0.168494941	0.428657284	0.006462263	Homo sapiens tubulin, beta 2A (TUBB2A), mRNA [NM_001069]
TUBB2B	chr6:3169809-3169750	0.275439519	0.163388644	0.286915192	0.040654721	1.041663132	0.964822468	0.019668205	1.90633 E-07	Homo sapiens tubulin, beta 2B (TUBB2B), mRNA [NM_001069]
TUBB2C	chr9:137413483-137413542	1.756253855	0.028564242	1.582950165	0.036152087	0.901321959	0.686052399	2.291435797	0.004324287	Homo sapiens tubulin, beta 2C (TUBB2C), mRNA [NM_006088]
TUBB2C	chr9:137413938-137413996	1.254805703	0.383709045	1.297507044	0.227619348	1.034030241	0.90101552	2.08304547	0.014414019	Homo sapiens tubulin, beta 2C (TUBB2C), mRNA [NM_006088]
TUBB3	chr16:88529436-88529495	1.400627824	0.01905224	1.051885025	0.818812703	0.751009659	0.236299682	1.236941281	0.121543798	Homo sapiens tubulin, beta 3 (TUBB3), mRNA [NM_006086]
TUBB3	chr16:88529938-88529997	3.034430862	0.008413314	1.200762639	0.641393838	0.395712637	0.056793328	1.056767975	0.804078784	Homo sapiens tubulin, beta 3 (TUBB3), mRNA [NM_006086]
TUBB4	chr19:64457044-6445645	1.53070267	0.03149165	1.34635951	0.050495638	0.879569584	0.42965393	0.66604622	0.095386797	Homo sapiens tubulin, beta 4 (TUBB4), mRNA [NM_006087]
TUBB4	chr19:6446948-6446889	0.863357155	0.673930756	0.374855762	0.032436531	0.434160717	0.068039613	0.168094436	0.001095585	(TUBB4), mRNA [NM_006087]
TUBB6	chr18:12315997-12316056	1.0407388	0.734339924	0.787111865	0.266446156	0.756301067	0.182486723	0.686841947	0.109123548	Homo sapiens tubulin, beta 6 (TUBB6), mRNA [NM_03225]

TABLE II. *Continued*

Gene name	Map position	DvM ^a linear ratio	DvM ^a <i>P</i> -value	AvM ^b linear ratio	AvM ^b <i>P</i> -value	AvD ^c linear ratio	AvD ^c <i>P</i> -value	TvM ^d Linear Ratio	TvM ^d <i>P</i> -value	Description
TUBB6	chr18:12316476-12316535	0.178899863	0.152612007	0.033417784	0.000983938	0.18679603	0.200910155	0.115261559	0.000208772	Homo sapiens tubulin, beta 6 (TUBB6), mRNA [NM_032525]
TUBB8	chr10:83404-83345	1.324871811	0.14689598	1.033948749	0.870229955	0.780414181	0.341973178	1.059355311	0.706490087	Homo sapiens tubulin, beta 8 (TUBB8), mRNA [NM_177987]
TUBD1	chr17:55292536-55292477	0.813032587	0.606588421	1.079556477	0.80028366	1.327814524	0.380245482	0.75772502	0.315577512	Homo sapiens tubulin, delta 1 (TUBD1), mRNA [NM_016261]
TUBE1	chr6:112502698-112502639	5.282486849	0.000264413	2.52173674	0.005352034	0.477376814	0.016883159	0.789883777	0.127356069	Homo sapiens tubulin, epsilon 1 (TUBE1), mRNA [NM_016262]
TUBG1	chr17:38018548-38018607	1.981144469	0.058338259	2.052718766	0.000182858	1.036127752	0.903060784	1.300489191	0.368611715	Homo sapiens tubulin, gamma 1 (TUBG1), mRNA [NM_001070]
TUBG2	chr17:38069000-38071031	1.677095651	0.074754047	1.651259413	0.000681646	0.984594654	0.948279178	1.161587557	0.597912576	Homo sapiens tubulin, gamma 2 (TUBG2), mRNA [NM_016437]
TUBGCP2	chr10:134986328-134986269	1.218542935	0.204636766	1.353312879	0.010136853	1.110599257	0.519396123	1.069323142	0.739996284	Homo sapiens tubulin, gamma complex associated protein 2 (TUBGCP2), mRNA [NM_006659]
TUBGCP3	chr13:112188148-112188089	1.873083313	0.011437334	1.775375299	0.023289891	0.947835735	0.835335934	2.393651106	0.002363706	Homo sapiens tubulin, gamma complex associated protein 3 (TUBGCP3), mRNA [NM_006322]
TUBGCP3	chr13:112188401-112188342	2.13005795	0.043459515	1.948168191	0.009516649	0.91460807	0.793708237	2.478424836	0.000169652	Homo sapiens tubulin, gamma complex associated protein 3 (TUBGCP3), mRNA [NM_006322]
TUBGCP3	chr13:112206955-112206334	4.316434459	0.002124934	4.104401538	1.760666 E-06	0.950877762	0.859372307	1.843666311	0.048125256	Homo sapiens tubulin, gamma complex associated protein 3 (TUBGCP3), mRNA [NM_006322]
TUBGCP5	chr15:20420386-20421393	2.190443907	0.016181992	2.373349141	0.011563644	1.083501446	0.557521077	1.677043363	0.144830062	Homo sapiens tubulin, gamma complex associated protein 5 (TUBGCP5), mRNA [NM_052903]
TUBGCP6	chr22:48959229-48959170	1.094052854	0.361173466	0.717879194	0.02461539	0.656165003	0.003882231	1.220462294	0.199609257	Homo sapiens tubulin, gamma complex associated protein 6 (TUBGCP6), transcript variant 2, mRNA [NM_001008658]

^aDiploid CRC cell lines us Normal colon mucosa.^bAneuploid CRC cell lines us Normal colon mucosa.^cAneuploid vs Diploid CRC Cell lines.^dCRC Tumors vs Normal colon mucosa.

MMR $-/-$ cells, it did not result in an increase in chromosome instability (data not shown).

The aneuploid colorectal cancers contain an intact DNA mismatch repair pathway (MMR+), but generally have loss of TP53 function. As such, the accumulation of genomic alterations primarily occurs through their inability to correctly respond to certain types of DNA lesions. This includes a failure to arrest the cell cycle and to activate the repair pathways necessary for proper repair of the damaged DNA. Such cells are also capable of altering the number of intact oncogenes and tumor suppressor genes via the gain and loss of chromosomes or chromosomal regions [Eshleman et al., 1998]. One potential mechanism for altering chromosome copy number is interference with the chromosome segregation machinery. Consistent with this idea was the presence of multiple γ -tubulin structures in the aneuploid colorectal cells that presumably represented functional centrosomes. We have now demonstrated that these extra structures contain a number of microtubule organizing center (MTOC) proteins considered to be the hallmark of functional centrosomes (i.e., γ -tubulin and PCNT) [Doxsey et al., 1994; Moritz et al., 1995]. The colocalization pattern of these proteins, as well as the cell-cycle dependent colocalization and redistribution of two kinases known to be involved in centrosome segregation and migration (i.e., PLK1 and AURKA), were identical in aneuploid and diploid CRC cell lines and in normal cells.

Further examination, however, revealed that these supernumerary structures did not behave like centrosomes. The presence of multipolar mitosis in the *Brcal* $-/-$ and *Tp53* $-/-$ MEFs, p53HCT116 and pancreatic tumor cell lines, all of which contained multiple γ -tubulin structures, was in sharp contrast to observations in the aneuploid CRC cell lines. The inability of the structures in the latter lines to nucleate α -tubulin containing microtubules, as revealed in our nucleation assays, provides one explanation. This is somewhat surprising given evidence that γ -tubulin is responsible for the nucleation activity of centrosomes [Mogensen et al., 1997].

Our dual immunocytochemistry/EM analysis revealed the presence of only one to two pairs of centrioles in most of the aneuploid CRC cells, despite the presence of multiple γ -tubulin structures. Even in SW837 where we observed multiple centrioles in an exceedingly low percentage of cells (Figs. 6I–6L), we did not observe more than two clusters of centrioles per cell. Thus, there appears to be a clear correlation between nucleation ability and the presence of centrioles in the tumor cell lines analyzed here. This is in contrast to observations in early mouse development and certain *Drosophila* cell lines, where centrosomes stripped of their centrioles have been shown to have nucleation activity [Debec et al., 1995]. It is also possible that nucleation from these structures occurs but is severely impaired, hence the inability of it to be detected in our assay.

Perhaps, modification of γ -tubulin is essential to its ability for nucleation [Khodjakov and Rieder, 2001]. Our colocalization studies indicate that two proteins (PLK1 and AURKA) whose modification of γ -tubulin is critical for progression through the cell cycle are associated with, and therefore in a position to modify, γ -tubulin in these nonfunctional structures [Feng et al., 1999]. Our analysis here of CRC cell lines, as well as of primary colon tumors (data not shown), confirms the findings of previous studies demonstrating elevated levels of these proteins in primary human colorectal cancers [Bischoff et al., 1998; Takahashi et al., 2000]. Although the protein concentrations and localization may be sufficient for the modification of γ -tubulin in the aneuploid cells, their enzymatic activity was not assessed. Analysis of *Xenopus* extracts has identified Xmap215 as a protein that is critical for the nucleation of mitotic spindles [Popov et al., 2002]. Perhaps, a failure of the human orthologous protein (CKAP5), which we observed to be significantly increased at the transcriptional level, to localize to the supernumerary, centriole-lacking structures is responsible for their inability to nucleate spindle formation.

Further, molecular interrogation of the differentially expressed genes identified through our analysis will be necessary to determine if they are in any way related to the functional capacity of γ -tubulin containing structures to nucleate mitotic spindles and form multipolar mitoses capable of causing chromosome missegregation. Overexpression of CSPP1, as occurs in the aneuploid CRC cell lines, has been shown to result in a cell cycle block at M and early G1 phases, with mitosis-arrested cells containing aberrant spindles [Patzke et al., 2005]. CETN2 localizes to spindles [Salisbury, 1995] and more recently has been found associated with the nuclear pore complex [Resendes et al., 2008] where it regulates mRNA and protein export into the cytoplasm. It has also been demonstrated to stimulate the early stages of nucleotide excision repair [Nishi et al., 2005] through its interaction with xeroderma pigmentosum group C protein (XPC1) [Popescu et al., 2003]. One of the γ -tubulin complex proteins, TUBGCP6, was expressed at lower levels in the aneuploid CRC cell lines. Because of its association with the γ -tubulin complex, a decrease in expression might explain the failure of the supernumerary structures in the CRC aneuploid cell lines to nucleate microtubules [Murphy et al., 2001].

Our results suggest the potential of antibodies against γ -tubulin or PCNT alone to be misleading, particularly when drawing inferences about the functionality of these structures. We have identified three distinct categories of tumor cells based on their centrosome number and functionality. The first contain a normal complement of functional centrosomes. This is exemplified by the near diploid colorectal tumors. The second consists of cells with supernumerary centrosomes that have nucleating capacity,

thereby resulting in active chromosome missegregation via multipolar mitoses. These would include the pancreatic tumor cell lines, *Brcal* and *Tp53*-deficient MEFs, *p53HCT116* and *Brcal*-deficient tumors [Xu et al., 1999; Weaver et al., 2002]. The degree of chromosomal instability in these cells may, however, depends on other factors such as the rate of missegregation and the fate of the daughter cells. The final series of cell lines, which includes the aneuploid colorectal cancer cell lines, have an abnormal distribution of centrosome-associated proteins, possibly through fragmentation of the pericentriolar matrix. Because the supernumerary structures were not capable of nucleating microtubules, and because multipolar mitoses were never observed, one might speculate that the consequence is an alteration of the functional capacity of "legitimate" centrosomes. As such, missegregation would result from a failure of sister chromatid separation rather than the active aberrant partitioning of chromosomes via attachment to the supernumerary centrosomes. Perhaps not surprisingly, these cell lines were no more karyotypically unstable than those cell lines containing a normal pair of centrosomes (data not shown).

In conclusion, the presence of γ -tubulin, pericentrin, and the modifying kinases PLK and AURKA are insufficient for the generation of a functional centrosome with the capacity to nucleate microtubules. Such supernumerary structures are therefore incapable of inducing the formation of multipolar mitoses; however, we cannot exclude a possible role in chromosome missegregation through disruption of the normal bipolar spindle. The assessment of centrosome function with respect to chromosome segregation must therefore take into consideration the presence of centrioles and the capacity to nucleate microtubules.

ACKNOWLEDGMENTS

The authors thank Kunio Nagashima for help with the EM analysis, Cristina Montagna for her insightful suggestions, Andre Nussenzweig and Curtis Harris for generously providing cell lines, and David Spector for critical reading of the manuscript.

REFERENCES

- Alieva IB, Uzbekov RE. 2008. The centrosome is a polyfunctional multi-protein cell complex. *Biochemistry (Mosc)* 73:626–643.
- Bischoff JR, Anderson L, Zhu Y, Mossie K, Ng L, Souza B, Schryver B, Flanagan P, Clairvoyant F, Ginther C, et al. 1998. A homologue of *Drosophila* aurora kinase is oncogenic and amplified in human colorectal cancers. *Embo J* 17:3052–3065.
- Boveri T. 1929. *The Origin of Malignant Tumors*. Baltimore: Williams & Wilkins.
- Bowerman B. 2004. Cell division: Timing the machine. *Nature* 430:840–842.
- Brinkley BR. 2001. Managing the centrosome numbers game: From chaos to stability in cancer cell division. *Trends Cell Biol* 11:18–21.
- Brinkley BR, Goepfert TM. 1998. Supernumerary centrosomes and cancer: Boveri's hypothesis resurrected. *Cell Motil Cytoskeleton* 41: 281–288.
- Bunz F, Dutriaux A, Lengauer C, Waldman T, Zhou S, Brown JP, Sedivy JM, Kinzler KW, Vogelstein B. 1998. Requirement for *p53* and *p21* to sustain G2 arrest after DNA damage. *Science* 282:1497–1501.
- Camps J, Grade M, Nguyen QT, Hormann P, Becker S, Hummon AB, Rodriguez V, Chandrasekharappa S, Chen Y, Difilippantonio MJ, et al. 2008. Chromosomal breakpoints in primary colon cancer cluster at sites of structural variants in the genome. *Cancer Res* 68:1284–1295.
- Camps J, Nguyen QT, Padilla-Nash HM, Knutson T, McNeil NE, Wangsa D, Hummon AB, Grade M, Ried T, Difilippantonio MJ. 2009. Integrative Genomics Reveals Mechanisms of Copy Number Alterations Responsible for Transcriptional Derepression in Colorectal Cancer Genes *Chromosomes Cancer* Aug 18 [Epub ahead of print].
- Debec A, Detraves C, Montmory C, Geraud G, Wright M. 1995. Polar organization of gamma-tubulin in acentriolar mitotic spindles of *Drosophila melanogaster* cells. *J Cell Sci* 108(Pt 7):2645–2653.
- Doxsey SJ, Stein P, Evans L, Calarco PD, Kirschner M. 1994. Pericentrin, a highly conserved centrosome protein involved in microtubule organization. *Cell* 76:639–650.
- Dufva M. 2009. Introduction to microarray technology. *Methods Mol Biol* 529:1–22.
- Erikson E, Haystead TA, Qian YW, Maller JL. 2004. A feedback loop in the polo-like kinase activation pathway. *J Biol Chem* 279: 32219–32224.
- Eshleman JR, Casey G, Kochera ME, Sedwick WD, Swinler SE, Veigl ML, Willson JK, Schwartz S, Markowitz SD. 1998. Chromosome number and structure both are markedly stable in RER colorectal cancers and are not destabilized by mutation of *p53*. *Oncogene* 17:719–725.
- Feng Y, Hodge DR, Palmieri G, Chase DL, Longo DL, Ferris DK. 1999. Association of polo-like kinase with alpha-, beta- and gamma-tubulins in a stable complex. *Biochem J* 339(Pt 2):435–442.
- Fukasawa K, Choi T, Kuriyama R, Rulong S, Vande Woude GF. 1996. Abnormal centrosome amplification in the absence of *p53*. *Science* 271:1744–1747.
- Ghadimi BM, Sackett DL, Difilippantonio MJ, Schrock E, Neumann T, Jauho A, Auer G, Ried T. 2000. Centrosome amplification and instability occurs exclusively in aneuploid, but not in diploid colorectal cancer cell lines, and correlates with numerical chromosomal aberrations. *Genes Chromosomes Cancer* 27:183–190.
- Glover DM, Leibowitz MH, McLean DA, Parry H. 1995. Mutations in aurora prevent centrosome separation leading to the formation of monopolar spindles. *Cell* 81:95–105.
- Gonda MA, Aaronson SA, Ellmore N, Zeve VH, Nagashima K. 1976. Ultrastructural studies of surface features of human normal and tumor cells in tissue culture by scanning and transmission electron microscopy. *J Natl Cancer Inst* 56:245–263.
- Hamanaka R, Smith MR, O'Connor PM, Maloid S, Mihalic K, Spivak JL, Longo DL, Ferris DK. 1995. Polo-like kinase is a cell cycle-regulated kinase activated during mitosis. *J Biol Chem* 270: 21086–21091.
- Hinchcliffe EH, Li C, Thompson EA, Maller JL, Sluder G. 1999. Requirement of Cdk2-cyclin E activity for repeated centrosome reproduction in *Xenopus* egg extracts [see comments]. *Science* 283:851–854.
- Jordan A, Hadfield JA, Lawrence NJ, McGown AT. 1998. Tubulin as a target for anticancer drugs: Agents which interact with the mitotic spindle. *Med Res Rev* 18:259–296.

- Kallioniemi A, Kallioniemi OP, Sudar D, Rutovitz D, Gray JW, Waldman F, Pinkel D. 1992. Comparative genomic hybridization for molecular cytogenetic analysis of solid tumors. *Science* 258:818–821.
- Khodjakov A, Rieder CL. 2001. Centrosomes enhance the fidelity of cytokinesis in vertebrates and are required for cell cycle progression. *J Cell Biol* 153:237–242.
- Lane HA, Nigg EA. 1996. Antibody microinjection reveals an essential role for human polo-like kinase 1 (Plk1) in the functional maturation of mitotic centrosomes. *J Cell Biol* 135:1701–1713.
- Lengauer C, Kinzler KW, Vogelstein B. 1998. Genetic instabilities in human cancers. *Nature* 396:643–649.
- Lingle WL, Lutz WH, Ingle JN, Maihle NJ, Salisbury JL. 1998. Centrosome hypertrophy in human breast tumors: Implications for genomic stability and cell polarity. *Proc Natl Acad Sci USA* 95:2950–2955.
- Mogensen MM, Mackie JB, Doxsey SJ, Stearns T, Tucker JB. 1997. Centrosomal deployment of gamma-tubulin and pericentrin: Evidence for a microtubule-nucleating domain and a minus-end docking domain in certain mouse epithelial cells. *Cell Motil Cytoskeleton* 36:276–290.
- Moritz M, Braunfeld MB, Sedat JW, Alberts B, Agard DA. 1995. Microtubule nucleation by gamma-tubulin-containing rings in the centrosome. *Nature* 378:638–640.
- Murphy SM, Preble AM, Patel UK, O'Connell KL, Dias DP, Moritz M, Agard D, Stults JT, Stearns T. 2001. GCP5 and GCP6: Two new members of the human gamma-tubulin complex. *Mol Biol Cell* 12:3340–3352.
- Neef R, Klein UR, Kopajtich R, Barr FA. 2006. Cooperation between mitotic kinesins controls the late stages of cytokinesis. *Curr Biol* 16:301–307.
- Nishi R, Okuda Y, Watanabe E, Mori T, Iwai S, Masutani C, Sugasawa K, Hanaoka F. 2005. Centrin 2 stimulates nucleotide excision repair by interacting with xeroderma pigmentosum group C protein. *Mol Cell Biol* 25:5664–5674.
- Patzke S, Hauge H, Sioud M, Finne EF, Sivertsen EA, Delabie J, Stokke T, Aasheim HC. 2005. Identification of a novel centrosome/microtubule-associated coiled-coil protein involved in cell-cycle progression and spindle organization. *Oncogene* 24:1159–1173.
- Petronczki M, Glotzer M, Kraut N, Peters JM. 2007. Polo-like kinase 1 triggers the initiation of cytokinesis in human cells by promoting recruitment of the RhoGEF Ect2 to the central spindle. *Dev Cell* 12:713–725.
- Pettersson E, Lundeberg J, Ahmadian A. 2009. Generations of sequencing technologies. *Genomics* 93:105–111.
- Pihan GA, Doxsey SJ. 1999. The mitotic machinery as a source of genetic instability in cancer. *Semin Cancer Biol* 9:289–302.
- Pihan GA, Purohit A, Wallace J, Knecht H, Woda B, Quesenberry P, Doxsey SJ. 1998. Centrosome defects and genetic instability in malignant tumors. *Cancer Res* 58:3974–3985.
- Popescu A, Miron S, Blouquit Y, Duchambon P, Christova P, Craescu CT. 2003. Xeroderma pigmentosum group C protein possesses a high affinity binding site to human centrin 2 and calmodulin. *J Biol Chem* 278:40252–40261.
- Popov AV, Severin F, Karsenti E. 2002. XMAP215 is required for the microtubule-nucleating activity of centrosomes. *Curr Biol* 12:1326–1330.
- Qian YW, Erikson E, Li C, Maller JL. 1998a. Activated polo-like kinase Plx1 is required at multiple points during mitosis in *Xenopus laevis*. *Mol Cell Biol* 18:4262–4271.
- Qian YW, Erikson E, Maller JL. 1998b. Purification and cloning of a protein kinase that phosphorylates and activates the polo-like kinase Plx1. *Science* 282:1701–1704.
- Resendes KK, Rasala BA, Forbes DJ. 2008. Centrin 2 localizes to the vertebrate nuclear pore and plays a role in mRNA and protein export. *Mol Cell Biol* 28:1755–1769.
- Ried T. 2009. Homage to Theodor Boveri (1862–1915): Boveri's theory of cancer as a disease of the chromosomes, and the landscape of genomic imbalances in human carcinomas. *EMM This issue* (pNA).
- Ried T, Heselmeyer-Haddad K, Blegen H, Schrock E, Auer G. 1999. Genomic changes defining the genesis, progression, and malignancy potential in solid human tumors: A phenotype/genotype correlation. *Genes Chromosom Cancer* 25:195–204.
- Rogers GC, Rogers SL, Schwimmer TA, Ems-McClung SC, Walczak CE, Vale RD, Scholey JM, Sharp DJ. 2004. Two mitotic kinesins cooperate to drive sister chromatid separation during anaphase. *Nature* 427:364–370.
- Salisbury JL. 1995. Centrin, centrosomes, and mitotic spindle poles. *Curr Opin Cell Biol* 7:39–45.
- Sato N, Mizumoto K, Nakamura M, Maehara N, Minamishima YA, Nishio S, Nagai E, Tanaka M. 2001. Correlation between centrosome abnormalities and chromosomal instability in human pancreatic cancer cells. *Cancer Genet Cytogenet* 126:13–19.
- Schröck E, du Manoir S, Veldman T, Schoell B, Wienberg J, Ferguson-Smith MA, Ning Y, Ledbetter DH, Bar-Am I, Soenksen D, et al. 1996. Multicolor spectral karyotyping of human chromosomes. *Science* 273:494–497.
- Stearns T. 2001. Centrosome duplication. A centriolar pas de deux. *Cell* 105:417–420.
- Takahashi T, Futamura M, Yoshimi N, Sano J, Katada M, Takagi Y, Kimura M, Yoshioka T, Okano Y, Saji S. 2000. Centrosomal kinases, HsAIRK1 and HsAIRK3, are overexpressed in primary colorectal cancers. *Jpn J Cancer Res* 91:1007–1014.
- Waldman T, Lengauer C, Kinzler KW, Vogelstein B. 1996. Uncoupling of S phase and mitosis induced by anticancer agents in cells lacking p21. *Nature* 381:713–716.
- Weaver Z, Montagna C, Xu X, Howard T, Gadina M, Brodie SG, Deng CX, Ried T. 2002. Mammary tumors in mice conditionally mutant for Brca1 exhibit gross genomic instability and centrosome amplification yet display a recurring distribution of genomic imbalances that is similar to human breast cancer. *Oncogene* 21:5097–5107.
- Xu X, Weaver Z, Linke SP, Li C, Gotay J, Wang XW, Harris CC, Ried T, Deng CX. 1999. Centrosome amplification and a defective G2-M cell cycle checkpoint induce genetic instability in BRCA1 exon 11 isoform-deficient cells. *Mol Cell* 3:389–395.
- Zhou H, Kuang J, Zhong L, Kuo W-L, Gray JW, Sahin A, Brinkley BR, Sen S. 1998. Tumor amplified kinase STK15/BTAK induces centrosome amplification, aneuploidy and transformation. *Nat Genet* 20:189–193.

Accepted by—
O. Olivero